U.S. DEPARTMENT OF THE INTERIOR
U.S . GEOLOGICAL SURVEY

INVESTIGATION OF THE SAN BRUNO FAULT NEAR THE PROPOSED EXTENSION OF THE BAY AREA RAPID TRANSIT LINE FROM COLMA TO SAN FRANCISCO INTERNATIONAL AIRPORT, SAN MATEO COUNTY, CALIFORNIA

by

U.S. Geological Survey

Open-File Report 97-429

Prepared in cooperation with the San Francisco Bay Area Rapid Transit District

1997

CONTENTS

FIGURES

INVESTIGATION OF THE SAN BRUNO FAULT NEAR THE PROPOSED EXTENSION OF THE BAY AREA RAPID TRANSIT LINE FROM COLMA TO SAN FRANCISCO INTERNATIONAL AIRPORT

EXECUTIVE SUMMARY

by
A. F. McGarr

Although never observed, the San Bruno fault has played a substantial role in numerous interpretations of the geology of the San Francisco peninsula since it was postulated by A.C. Lawson (1895). As represented by Bonilla (1971), the San Bruno fault is only inferred, with a trace that extends in a northwest-southeast direction along the center of Colma Valley, approximately parallel to the San Andreas fault and about 4 kilometers to the northeast. Because this inferred fault trace nearly coincides with the alignment of the proposed Bay Area Rapid Transit (BART) extension from Colma to the San Francisco International Airport (SFO), with multiple intersections between the alignment and the trace, it was clearly advisable to reassess the possible hazard to engineered structures posed by this enigmatic fault using the most up-to-date geophysical, geotechnical, and geological information, as well as state-of-the-art interpretive techniques.

Accordingly, at the request of BART, the U.S. Geological Survey (USGS) performed a three-part investigation for the purpose of determining whether or not the San Bruno fault exists and, if so, whether it is active. As summarized here and described in more detail in the individual reports, none of these investigations found any positive evidence supporting the existence of the San Bruno fault, much less any recent offset.

Part A: Geophysical Investigation

This effort entailed the analysis and interpretation of a detailed gravity survey, conducted in 1989, and a high-resolution aeromagnetic survey flown during March 1995. In the Colma Valley, low-density, nonmagnetic sediments of the Merced and Colma formations overlie the higher density, Franciscan bedrock which contains widespread magnetic bodies. If the San Bruno fault exists and is of any consequence, then it must have substantially offset the Franciscan bedrock in a dip-slip (vertical) and/or strike-slip (horizontal) sense.

By virtue of the density contrast between the sediments and the bedrock, the gravity data can be used to map the buried bedrock topography to relatively high resolution, including any vertical offsets due to faulting. At a resolution of 15 to 30 meters, the gravity data show no evidence of any dip-slip offsets in the vicinity of the San Bruno fault trace.

The aeromagnetic data, which are best suited for identifying strike-slip faults, show aligned magnetic boundaries for the known mapped faults in the area of this study, including the Hillside and San Andreas faults. No such alignment was detected in the vicinity of the San Bruno fault trace. Thus, the aeromagnetic data provided no positive evidence for the existence of the San Bruno fault. Evidence arguing against the existence of the San Bruno fault is provided by a subtle magnetic anomaly that crosses the inferred fault trace. The absence of any apparent offset of this anomaly limits any possible strike-slip displacement to, at most, 1 to 2 kilometers.

Part B: Digital Geomorphic Investigations

The analysis of digitized topographic maps can reveal subtle topographic features indicative of recent fault slip. Maps of slope, curvature, and shaded relief are especially useful for this purpose. In the region between Colma and SFO, however, development has long since altered parts of the land surface, thereby imposing artificial elements in modern topographic data. Accordingly, detailed topographic maps made by the U.S. Coast Survey during the 1852-1869 period were digitized for this analysis.

Neither the digital elevation map of the 1800s topography nor any of the derivative maps (slope, curvature, or shaded relief) produced from these data yielded any linear features diagnostic of recent faulting near the inferred San Bruno fault trace. Similarly, topographic profiles measured at right angles to the fault trace show no indication, such as a systematic change in slope, of a recent active fault. Moreover, the stream channels that cross the inferred fault trace show no detectable lateral offset, which argues against any recent strike-slip faulting. In short, a high-precision digital analysis of the unmodified topography failed to yield any indication of recent faulting.

Part C: Analysis of Subsurface Data

This investigation was based primarily on information from borings and cone penetration tests made along the Colma to SFO alignment that were provided by BART. This comprehensive, although shallow-level, data set yielded the most detailed geologic cross section. Two sections perpendicular to the inferred fault were made from borings that were much more widely spaced and of lower quality data . The results of this study indicate substantial lateral variation in the near-surface geology of the Colma Formation to the extent that, even for borings separated by 100 meters, or so, correlations of lithologic units (e.g. sand, clay, gravel) between holes is difficult. Nonetheless, reasonable correlations show overlapping geologic units that nearly preclude any substantial dip-slip faulting along the section of the BART alignment that was studied. Before this study, a reported change in the lithology of the Colma formation, between borings that straddle the position where the inferred fault intersects the BART alignment, could be taken as possible evidence of a fault offset. It now seems, however, that this lithologic change simply reflects normal variability within the Colma. Thus, the subsurface data do not suggest the existence of the San Bruno fault.

In summary, we find no evidence for the existence of the San Bruno fault as a mappable geologic structure or as a source of earthquakes or fault displacement.

INTRODUCTION

Geologic maps of the San Francisco South quadrangle (Bonilla, 1971), and the San Mateo quadrangle (Pampeyan, 1994) show a hypothetical fault, the San Bruno fault, that extends southeastward from Lake Merced on the northwest, down the center of Colma Valley, to the vicinity of San Francisco International Airport and slightly beyond (fig. A-1). The San Bruno fault, as shown on these maps, lies close to, and in places intersects, the right-of-way along which the Bay Area Rapid Transit District (BART) proposes to extend the rail line from Colma to the San Francisco International Airport and Millbrae (BART-SFO). A potentially active fault located as shown on the geologic maps of the San Francisco South and San Mateo quadrangles could pose a threat to the BART extension.

The U.S. Geological Survey review of the Draft Environmental Report on the proposed extension of BART indicated that the existence and age of the San Bruno fault were equivocal, and contained the following statement: "...mitigation measures should include a search for evidence of the San Bruno fault and its recency of activity by (1) a geological examination and interpretation of borehole data that have been and will be acquired for the project, and(2) geological examination of all cuts made during construction of the project." (Taylor, 1995). In transmitting the review to the Federal Transit Administration, the Department of the Interior requested that the mitigation measures be adequately documented in the Supplemental Draft Environmental Statement (Taylor, 1995). BART then contacted the USGS in Menlo Park regarding cooperation.

During discussions between BART and the USGS, BART indicated that the proposed examination of cuts during construction of BART-SFO would be very limited because of methods of construction and time constraints. The USGS noted that the change in character of the Colma Formation at Chestnut Avenue reported by Geotechnical Consultants, Inc. (1995, p. 15) is the place where the hypothetical San Bruno fault as shown by Bonilla (1971) crosses the BART alignment. The discussions also revealed that existing unpublished and unstudied topographic and geophysical information would be very useful in answering the questions about the San Bruno fault. Consequently, BART and the USGS signed an agreement on May 17, 1996, whereby the USGS would carry out a three-part investigation of the San Bruno fault consisting essentially of 1) preparation of geologic cross-sections using subsurface data obtained from BART and other sources; 2) analysis of recently-acquired gravity and magnetic data; and 3) a geomorphological study using large-scale topographic maps made in the 1800s and computer analysis of the digitized topography. Draft reports on these investigations were given to BART in September, 1996. Comments received from BART in December, 1996, were minor except for requested changes in the format, which are incorporated in the present report. Although the investigations, designated A, B, and C, are individually authored to establish primary responsibility, the investigators met frequently to discuss progress and results of the work, and all coauthors agree with the conclusions. In addition, Carl Wentworth, who played the major role in the difficult conversion of the 1800s topographic maps to digital form (Wentworth and others, unpub. data, 1996), was an active participant in the discussions, and agrees with the conclusions.

Geomorphic investigation of the San Bruno fault was not limited to the study of digititized versions of old maps (Part B of this report). Stereographic aerial photographs flown in 1943 and 1946 were examined by M.G. Bonilla for geomorphic evidence of faulting. A search was made for old photography, including the indexes of Fairchild Aerial Surveys coverage, but none was found that significantly predates the 1943 photography in the critical area southwest of San Bruno Mountain. Correspondence with the U.S. Geological Survey Photographic Library and the Library of Congress revealed that their files contain no pre-urbanization low-oblique or ground-based photographs of the critical area. Prints made from glass plates of published and unpublished 1906 photos from the State Earthquake Investigation Commission collection, obtained by C.S. Prentice of USGS from the files of the Bancroft Library in Berkeley, were examined by Bonilla, who found no evidence in them suggestive of faulting.

For brevity, the hypothetical San Bruno fault is referred to in this report as "the San Bruno fault."

Figure A-1. Index map of the San Bruno fault and vicinity. SFO, San Francisco International Airport. Proposed BART extension includes several alternatives near SFO. Features named on this map appear on figures A-2 through A-4, but are not named.

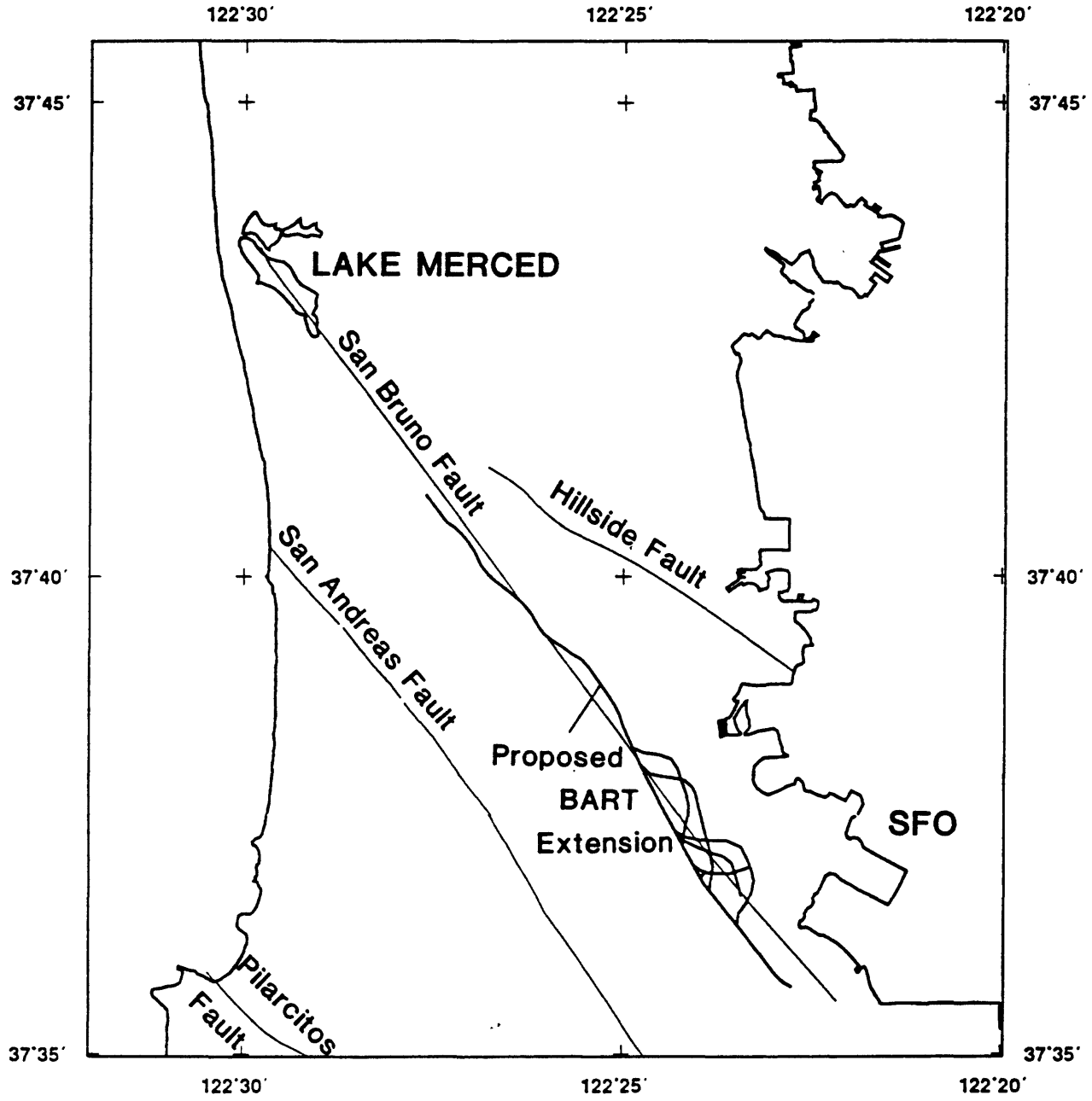
122°30'
122°25'
122°20'
37°45'
37°40'
37°35'
LAKE MERCED
San Bruno Fault
Hillside Fault
San Andreas Fault
Proposed
BART
Extension
SFO
Pilarcitos
Fault

Figure A-1

A. GEOPHYSICAL INVESTIGATION

by
Robert C. Jachens

INTRODUCTION

At the request of BART a geophysical investigation of the San Bruno fault was begun in 1996. The purpose of this study was to determine whether there is geophysical evidence that would support the existence of the San Bruno fault and, if so, that would better define the location of the fault. This report describes the analysis and interpretation of detailed gravity data and high-resolution aeromagnetic data from the vicinity of the San Bruno fault.

BASIC PRINCIPLES

Measurements of gravity at the land surface commonly are used to define lateral density variations caused by subsurface lateral changes in rock type or structure (Dobrin and Savit, 1988; Telford and others, 1976). In areas such as the Colma Valley where young, low-density sedimentary deposits (Merced and Colma formations, densities typically less than 2.2 g/cm^3) overlie dense buried rocks (Franciscan Complex, densities typically greater than 2.65 g/cm^3), detailed gravity surveys are effective in determining the thickness of the sedimentary deposits and especially in defining any abrupt lateral changes in the thickness of these deposits (see Bonilla, this report, for a more detailed description of the local geology). For the present study, any fault that a) was active following the onset of deposition of the Merced and Colma Formations and b) experienced movement that resulted in either real or apparent vertical offset of more than a few tens of meters across the fault, should produce a characteristic gravity anomaly (local distortion in the Earth's gravity field). Such anomalies can be analyzed to define the position of the fault and the magnitude of the vertical offset.

Areal measurements of the Earth's magnetic field, made either at the ground surface or from a low-flying aircraft, commonly are used to map lateral variations in the quantity and distribution of magnetic minerals (mostly magnetite) in the underlying rocks (Dobrin and Savit, 1988; Telford and others, 1976). Abrupt lateral changes in the distribution of magnetic minerals, which often accompany abrupt lateral changes in rock type, produce characteristic magnetic anomalies (local distortions of the Earth's magnetic field) that can be analyzed to determine the locations of the magnetic boundaries.

In the general vicinity of the San Bruno fault, magnetic rocks are confined to the Franciscan Complex that outcrops or underlies surface rocks at shallow depth. These magnetic rocks are widespread at depth and include, primarily, serpentinites and metamorphosed basalts. Nonmagnetic rocks such as sandstones also make up parts of the Franciscan Complex. An important characteristic of the magnetic Franciscan rocks, at least for the purposes of the present study, is that the magnetic properties are not uniform with respect to a given rock type, or even uniform within any individual rock body. Commonly, magnetizations within these types of rocks can vary smoothly from one part of a rock body to another by factors of 2 or more. Thus, the buried rocks in the vicinity of the San Bruno fault present a magnetic image characterized by smoothly varying distributions of magnetization punctuated occasionally by abrupt boundaries at the edges of rock bodies, and interspersed with nonmagnetic bodies, all the result of complex processes that attached fragments of old oceanic crust to the edge of the continent and

metamorphosed it to varying degrees. The resulting irregular distribution of magnetization within these rocks is reflected directly in magnetic anomalies measured near the Earth's surface.

The Franciscan rocks with magnetic characteristics as described above present an ideal situation for identifying, by means of magnetic surveys, strike-slip faults that have offset the subsurface rocks. First, because of the pervasive and irregular distribution of magnetization within the "unfaulted" Franciscan rock bodies, any fault across which substantial strike-slip offset has occurred is almost certain to have juxtaposed rocks with differing magnetizations along much of its length. Because the consequent magnetic boundaries can be located by analysis of a magnetic map, possible strike-slip faults can be identified by searching for aligned magnetic boundaries. Second, active and ancient fault zones throughout the Franciscan terranes of the California Coast Ranges commonly are observed to have sheet-like bodies of serpentinite entrained along them. Because serpentinite is strongly magnetic, these faults zones are characterized by long, narrow magnetic highs that can be readily identified on magnetic maps. Faults with predominantly dip-slip offset can sometimes be identified on the basis of analyses of magnetic maps, but they tend to be more difficult to identify than strike-slip faults.

DATA

Gravity Data

A detailed gravity survey (fig. A-2) of the area including the San Bruno fault and vicinity as far south as roughly the San Francisco International Airport was conducted in 1989 for the purpose of defining the thickness of sediments of the Merced and younger formations comprising the groundwater basin beneath western San Francisco and cities to the south (Roberts, 1991). Station spacing of approximately 0.4 km was maintained wherever possible. The data were reduced using standard procedures (Roberts, 1991) and converted to residual anomalies in order to emphasize the gravity anomalies reflecting shallow density distributions, those of interest to the groundwater study and to the present study as well. Typical uncertainties associated with these data arising from uncertainties in station elevation, location, observed gravity, and terrain corrections, are estimated to be 0.1 mGal or less (see accuracy codes in Roberts, 1991).

Magnetic Data

A high-resolution aeromagnetic survey of the central San Francisco Bay area and vicinity was flown on contract to the U.S. Geological Survey during March 1995. The purpose of the survey was to provide information on the concealed faults of the San Andreas system as part of the U.S. Geological Survey's Earthquake Hazards Reduction Program. Total field magnetic data were collected with a fixed-wing aircraft along NE-SW oriented flightlines spaced 0.5 km apart and controlled by a precise GPS navigation system. The survey aircraft maintained a nominal height of 250 m above the surface in water-covered areas and 300 m above the land surface in developed onshore areas. Because of extreme topographic relief in some places, the aircraft was not always able to maintain a constant altitude above the land surface and typically passed closer to the ridge tops than to the bottoms of the intervening valleys. Data were measured about every 45 m along the flightlines.

The magnetic data were corrected for diurnal fluctuations of the Earth's field, and the International Geomagnetic Reference Field, updated to the dates of the survey, was subtracted from the observations to yield residual magnetic data (total field magnetic anomaly). The residual magnetic field values were interpolated to a square grid (grid spacing=100 m; projection=Universal Transverse Mercator, central meridian=123° W., base latitude=0°) by a process based on the

principle of minimum curvature (Briggs, 1974). The part of this survey covering the present study area is shown in figure A-3.

A small area including parts of the top of San Bruno Mountain (see white area near the center of figure A-3) was not covered as part of the survey described above because electronic transmission towers and other tall antennas posed a hazard to the survey aircraft. Although the San Bruno fault as proposed does not pass through this area, the nearby Hillside fault (fig. A-3) does pass through the southern part of the survey hole. Because this fault is potentially important in understanding the setting of the San Bruno fault, ground magnetic measurements every 30 m were made along two profiles extending south from the crest of San Bruno Mountain (fig. A-3) inside the survey hole.

DATA ANALYSIS

Gravity Data

The gravity data were used to estimate the thickness of Merced formation and younger deposits throughout the study area by means of a slight modification of a procedure developed by Jachens and Moring (1990). In this procedure the position of the surface of the Franciscan rocks determined from outcrops and wells is used to separate the residual gravity field into two components, one caused by the low density sedimentary deposits and the other due to density variations within the Franciscan Complex and deeper parts of the crust and mantle. The gravity component caused by the low-density sedimentary deposits is then used to calculate the thickness of those deposits throughout the study area, a calculation that is controlled by an assumed density contrast between these deposits and the underlying rocks. This entire procedure was carried out using calculation grids 200 m on a side. The spatial resolution of the resulting calculated distribution of sediment thickness (fig. A-4) is no finer than the spacing of the original gravity data, about 0.4 km. Although this resolution is too coarse to satisfy all the requirements of the present study, the map of sediment thickness (fig. A-4) does highlight the major features of the sedimentary basin beneath western San Francisco, and places the proposed San Bruno fault in a broader context.

Magnetic Data

The magnetic survey data received from the contractor includes a number of local anomalies produced by manmade structures containing a significant amount of steel. This type of anomaly tends to interfere with the recognition of anomalies caused by magnetic rocks, especially where the natural anomalies are weak. Therefore, an attempt was made to eliminate the "cultural" anomalies from the magnetic data set near the San Bruno fault before proceeding with the interpretation. To accomplish this, I identified all local anomalies within a 3-km-wide swath centered on the San Bruno fault and having specific characteristics suggestive of a cultural source (most important, a wavelength appropriate for a source located at the ground surface directly beneath the aircraft, but also including high amplitude, presence on only one flight line, and an indication of a large structure at the appropriate location on the topographic map). Each of the possible sites was visited personally to determine if a candidate structure was present. Of the 12 sites identified, only one seemed to lack an appropriate candidate structure. Ones that were identified included the BART parking structure adjacent to Woodlawn Cemetery, the parking structure/terminal building and the United Airlines maintenance facility buildings at San Francisco International Airport, high-rise buildings, hospitals, and large warehouses. For those anomalies where a cultural source was identified, theoretical modeling of the magnetic field of the source was used to delineate the section of the observed data along each profile likely to be perturbed by the cultural anomaly, and the data for these sections was simply discarded. The resulting map is shown in figure A-3.

The modified aeromagnetic data were then analyzed by an objective procedure designed to locate the edges of magnetic rock bodies (shown by aligned "+" symbols on figure A-3) based on the magnetic anomalies they produce. These locations were determined by means of a numerical technique applied to the magnetic data that is a slight modification of a technique proposed by Cordell and Grauch (1985) and implemented by Blakely and Simpson (1986). The original technique is a process for locating the edges of magnetic bodies which makes use of a linear filter, the pseudogravity transform (Baranov, 1957), which converts a magnetic anomaly to an equivalent gravity anomaly. In the same way that the maximum horizontal gradients of a gravity anomaly produced by a shallowly buried body lie nearly over the edges of the body, especially if the sides dip steeply, the maximum horizontal gradients of a pseudogravity anomaly define the edges of the magnetic body that cause the magnetic anomaly. For the present study, I modified the edge-locating procedure slightly by applying the technique, not to the simple pseudogravity transformation of the San Francisco Bay area magnetic data, but rather to the difference between the transformed magnetic data and those same data continued upward 100 m. Upward continuation of potential field data suppresses the shorter wavelength components of an anomaly, such as are produced by the shallowest parts of a body, at the expense of the longer wavelength components (Blakely, 1995) that reflect the deeper parts of the body. By applying the edge-locating technique to the difference, I focused the procedure on the shallowest parts of the magnetic bodies, the top edges.

INTERPRETATION

Gravity Interpretation

The primary reason for interpreting the gravity data as part of this study is to search for vertical offset of the surface of the Franciscan rocks that might be associated with past movement on the San Bruno fault. Evidence of vertical offset of the Franciscan rock surface in the appropriate location could provide support for the existence of the San Bruno fault and help define its position. I examined the gravity data in three different, but related, ways to search for possible fault-related offset of the Franciscan rock surface in the vicinity of the San Bruno fault: 1) examination of the inferred three-dimensional geometry of the depth to Franciscan rock beneath Colma Valley (fig. A-4) in search of abrupt lateral changes in this depth possibly related to faulting; 2) detailed examination of a 2-dimensional gravity model of the Franciscan rock surface along a profile crossing the proposed location of the San Bruno fault for which I have particularly good gravity coverage; and 3) examination of a set of gravity profiles (perpendicular to the fault throughout the area of interest) for anomalies with the characteristic shape and amplitude that would be produced by a vertical offset of the Franciscan rock surface.

Figure A-4 shows the depth to Franciscan rocks beneath Colma Valley and surrounding areas inferred from the gravity data and constrained by the distribution of outcrops of Franciscan rock and by wells that penetrated these rocks at depth. The most prominent feature on this map is the deep basin aligned along the San Andreas fault. This basin, more than 1 km deep and about 3 km wide near the coast, both narrows and shallows to the southeast. The basin is bounded on the southwest by the San Andreas fault and marked on the northeast by a zone of closely spaced contours (A on figure A-4), possibly indicating a fault, that lies just south of Lake Merced near the coast and converges south-southeast toward the San Andreas fault. By contrast, the San Bruno fault is not centered on nor aligned along a zone of closely spaced depth contours, such as might be expected if the fault accommodated significant vertical offset of the Franciscan rock surface.

In order to search in more detail for evidence of vertical offset on the San Bruno fault, I constructed a 2-dimensional gravity model (Fig A-5a) normal to the fault along a profile for which

closely spaced gravity data are available (fig. A-2). This model shows a steeply northeast-dipping basin edge at the San Andreas fault and an abrupt southwest facing step in the surface of the Franciscan rock approximately 1.5 km northeast of the San Andreas fault that probably also is a fault. The model indicates no offset greater than 15 m in the surface of Franciscan rock beneath the San Bruno fault or within a kilometer of it in either direction. Based on the reliability of the gravity data and the closeness of the model fit to the observed data, any localized offset of the Franciscan rock surface accommodating 15 m or more of vertical separation should have been detected during this modeling.

Finally, five gravity profiles (g1-g5) normal to the San Bruno fault along the proposed BART extension (see figure A-2 for locations) were extracted from the gravity data used to construct figure A-2 and examined for any characteristic gravity anomaly that might indicate an offset in the surface of Franciscan rock beneath the fault trace. These profiles are shown in the upper panel of figure A-5b, registered with respect to the profile location of the San Bruno fault. For comparison, the gravity anomaly expected from a 60 m vertical step in the surface of Franciscan rock (at roughly the depth of Franciscan rock beneath the San Bruno fault, from figure A-4) is shown in the bottom panel. It too is registered to the profile location of a step beneath the trace of the San Bruno fault. To first approximation, for steps of different magnitude the shape of the gravity anomaly will be the same as shown in figure A-5b, but the amplitude of the anomaly will be the amplitude shown in the lower panel of figure A-5b multiplied by the ratio [(actual amplitude)/60 m].

No anomalies like that shown in the bottom panel of figure A-5b centered on the fault location are apparent on any of the five profiles shown. It is difficult to identify any such anomaly even half the amplitude of the one associated with a 60 m step, although attempting to isolate the anomaly from a 30 m step on every profile probably is at about the limit of the data reliability.

Magnetic Interpretation

As mentioned in the section titled "Basic Principles", the magnetic data are best suited for identifying strike-slip faults, and such faults often can be located by aligned magnetic boundaries. For example, much of the 3 km-long mapped trace of the Hillside fault (fig. A-3) coincides with magnetic boundaries (indicated by the small "+" symbols on figure A-3) located by the automated procedure described in the section titled "Data Analysis". Furthermore, the linear magnetic boundary that continues on strike 6 km northwest from the northwest tip of the mapped Hillside fault (marked by the nearly straight line of "+" symbols connecting the fault tip with the southwest shore of Lake Merced) most likely marks the northwest extension of the Hillside fault into the area where it is concealed by young alluvium and, thus, not directly mappable. As another example, the 4.5-km-long reach of the San Andreas fault closest to the coast is associated with a parallel magnetic boundary marked by the line of "+" symbols arrayed 200-300 m northeast of the fault trace. The systematic displacement of the magnetic boundary from the mapped fault trace is most likely caused by a northeast dipping fault plane along this reach, as was found in the detailed gravity model (fig. A-5a). The onshore San Andreas fault-related magnetic boundary projects on strike an additional 5 km offshore, where it clearly defines the straight, northeast edge of a large magnetic block. The offshore boundary most likely marks the location of the San Andreas fault offshore, an area where it is concealed by water. Farther southeast, the San Andreas fault is not as well defined magnetically, but segments of magnetic boundaries do lie along the fault (fig. A-3) and no major magnetic anomalies cross the fault. Therefore, the magnetic data are compatible with the San Andreas fault within the study area being a major strike-slip fault with substantial offset. Finally, other important strike-slip faults in the San Francisco Bay area, including the Hayward and

Pilarcitos faults (a short segment of which is shown on figure A-3), coincide with clearly-defined magnetic boundaries (Brabb and Hanna, 1981; Jachens and others, unpub. data, 1996).

In contrast to the faults described above, the hypothetical San Bruno fault (fig. A-3) is not associated with any long, straight magnetic boundaries, nor with a consistent set of shorter, aligned magnetic boundary segments. This is especially true along the length of the proposed BART extension (fig. A-3). A straight, 4 km-long, well-defined magnetic boundary (B on figure A-3) does lie between the central part of the Hillside fault and the San Bruno fault (fig. A-3), but this feature is located 0.5-1.5 km northeast of the San Bruno fault (and the location of the proposed BART extension), and is parallel to the Hillside fault, not the San Bruno fault. It does not intersect the location of the proposed BART extension. The northeastward decreasing magnetic field strength between the San Bruno fault and feature B (fig. A-3) does not reflect a dipping magnetic interface, but rather is the expected shape of the northeastern part of a magnetic anomaly produced by a magnetic body at this latitude having a flat upper surface. Another straight, 5 km-long magnetic boundary (C on figure A-3) lies about midway between the San Andreas fault and the San Bruno fault, adjacent to the northwestern half of the proposed BART extension. This boundary lies approximately 1.5 km southwest of the proposed BART extension and does not intersect it.

The discussion of the magnetic data to this point has focused on a search for evidence of the existence of the San Bruno fault as shown by Bonilla (1971) and such evidence was not found. The magnetic data also might be able to provide evidence that would directly argue against the existence of the San Bruno fault, at least as a fault that has accommodated significant strike-slip offset. This evidence would be in the form of anomalies (and, therefore, magnetic rock bodies) that cross the hypothetical fault without being offset. The only magnetic anomaly on figure A-3 that might be used as evidence against the San Bruno fault being a major strike-slip fault is the crudely "L"-shaped magnetic high (the magnetic high confined between magnetic boundaries B and C, highest part greater than -40 nT) whose crest lies southwest of the northern third of the proposed BART extension. The magnetic body causing this anomaly crosses the San Bruno fault and extends to the northeast at least as far as the well-defined magnetic boundary located about midway between the Hillside and San Bruno faults and discussed in the previous paragraph. The southeast flank of this body, although oriented nearly normal to the San Bruno fault, is only poorly defined magnetically (by the -40 and -50 nT contours). The diffuse nature of this boundary may reflect a smooth decrease in magnetization to the southeast, or an extremely shallowly-dipping southeast contact between bodies with different magnetizations. In either case, the magnetic map indicates that this boundary has not been offset laterally along the San Bruno fault by more than 1-2 km, and contains no evidence that it has been offset at all.

CONCLUSIONS

Detailed gravity data and high-resolution magnetic data covering the Colma Valley were examined for any evidence that might support the existence of the hypothetical San Bruno fault, and no such evidence was found. The absence of any characteristic gravity anomalies in the vicinity of the San Bruno fault argues against any vertical offset of more than 15-30 m of the buried surface of Franciscan rock beneath the fault trace. Similarly, the absence of linear magnetic boundaries aligned along the San Bruno fault, even in the presence at depth of a Franciscan Complex block pervasively riddled with magnetic rock bodies, argues against any substantial strike-slip offset across this fault. Maximum strike-slip offset across the San Bruno fault is weakly constrained to

be less than approximately 1-2 km by the apparent lack of offset of a poorly resolved magnetic feature that crosses the fault.

None of the statements in the preceding paragraph proves that the San Bruno fault does not exist. However, no geophysical evidence for its existence as a moderately-dipping, steeply-dipping, or vertical structure was found in a careful search.

Figure A-2. Map showing isostatic residual gravity of the study area. "+" symbols indicate locations of gravity observations. Profiles: sf-2, 2-dimensional gravity model shown in figure A-5a; g1-g5, locations of gravity profiles shown on figure A-5b. Faults and cultural features named on figure A-1. Contour interval + 2 mGal.

ISOSTATIC RESIDUAL GRAVITY

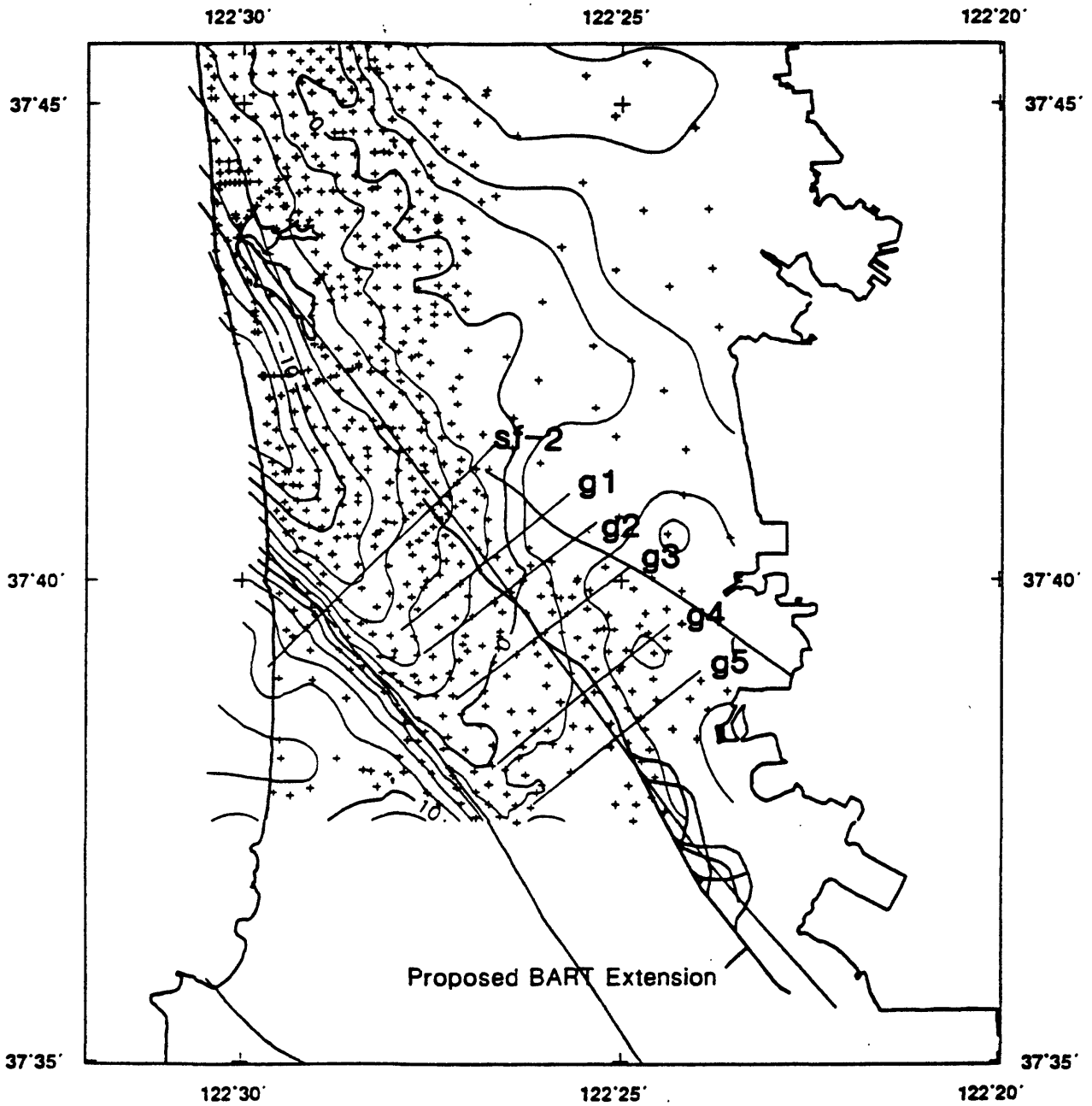

Contour Interval 2 mGal

Figure A-2

Figure A-3. Aeromagnetic map of the study area. "+" symbols indicate the locations of magnetization boundaries, determined by the objective procedure described in the section titled "Data Analysis". Two magenta triangles (at south edge of data hole in center of map) indicate magnetization boundaries determined from ground profiles (shown as irregular, roughly north-south lines passing through the triangles). Faults and cultural features named in figure A-1. Contour interval = 10 nanoTeslas (nT).

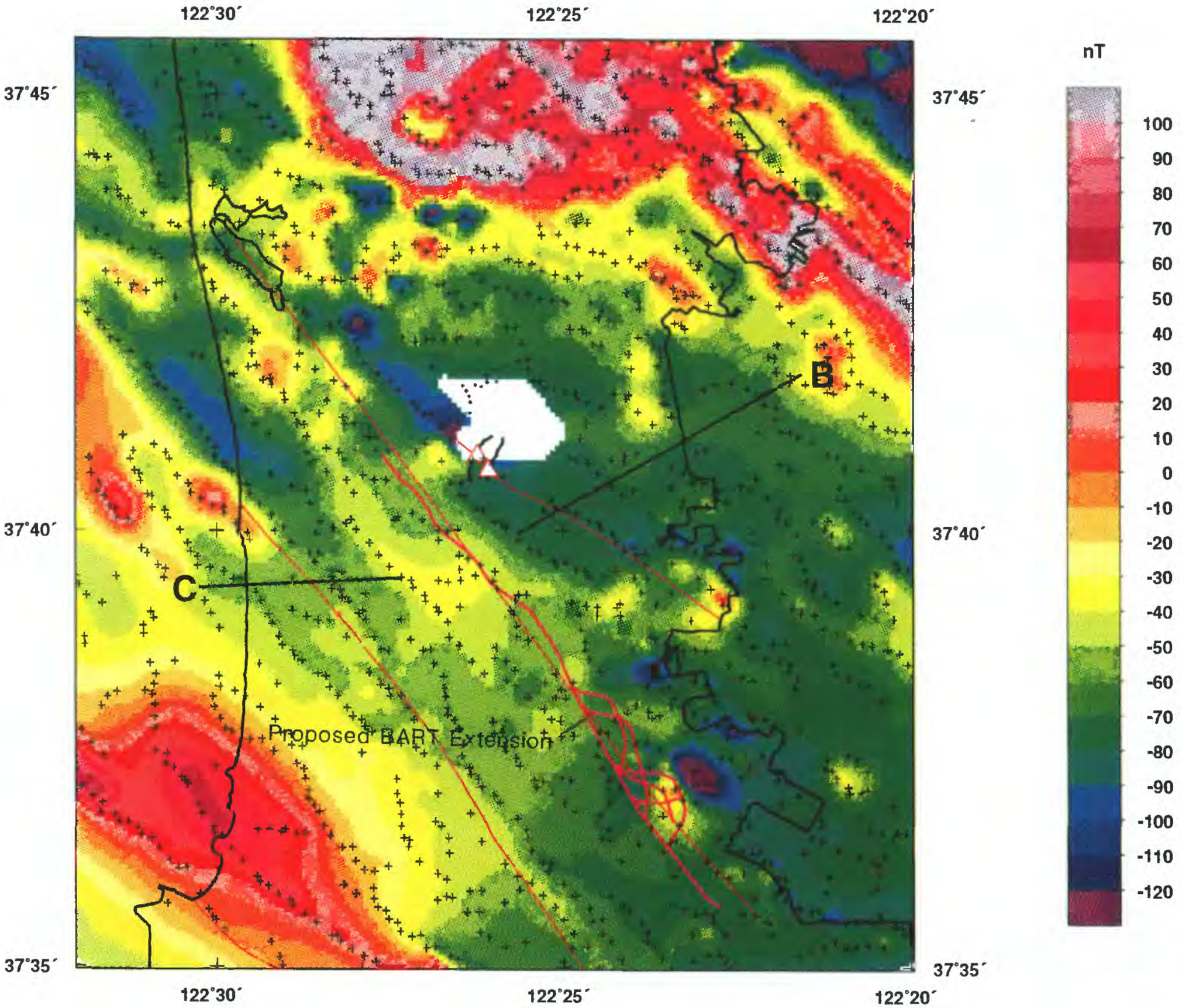
122°30´
122°25´
122°20´
37°45´
37°40´
37°35´
B
C
Proposed BART Extension
nT
100
90
80
70
60
50
40
30
20
10
0
-10
-20
-30
-40
-50
-60
-70
-80
-90
-100
-110
-120
0 1 2 3 4 5 6 7 8 9 10 KM

Figure A-3

Figure A-4. Depth to the surface of Franciscan rocks (in kilometers) inferred from the gravity data constrained by Franciscan outcrop patterns, wells that penetrated Franciscan rocks at depth , and an assumed density/depth function. Contour interval 0.1 km. Hachures point in direction of increasing depth. Faults and cultural features named on figure A-1. The contours outline a narrow basin approximately 1.2 km deep and bounded on the southwest by the San Andreas fault. The steeply-dipping northeast flank of the basin (indicated by "A") possibly also is fault controlled.

DEPTH TO FRANCISCAN ROCKS

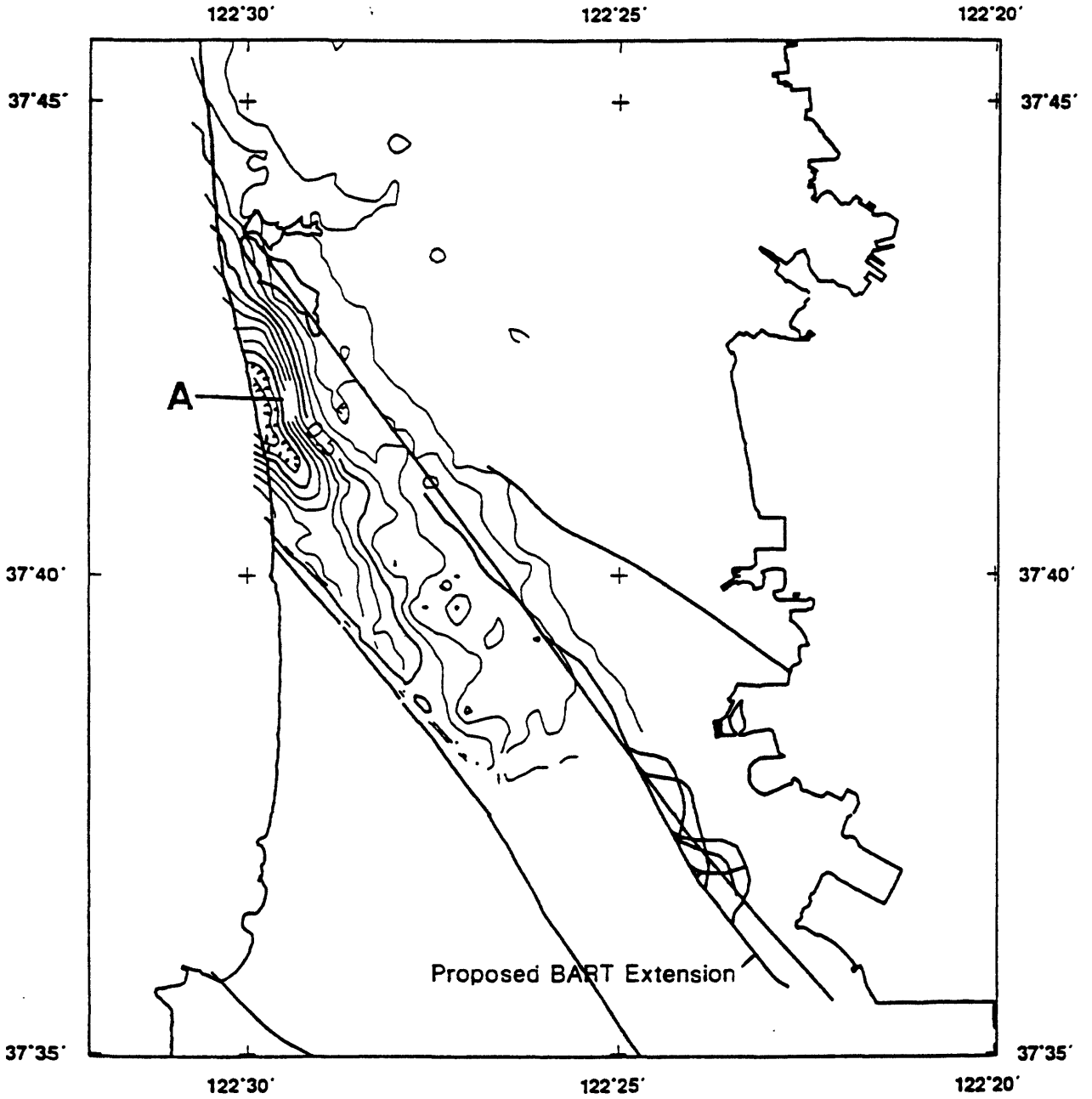

Contour Interval 100 m

Figure A-4

Figure A-5a. Two-dimensional gravity model along profile sf-2 (see figure A-2 for location) showing the depth to Franciscan rock beneath Colma Valley and the lack of any recognizable vertical offset of its surface associated with the San Bruno fault. Open circles in upper panel indicate actual gravity station values, projected normal to the profile strike direction. Line in upper panel indicates theoretical gravity calculated from the model shown in the lower panel. Density contrasts (with respect to Franciscan Complex sandstones, 2.67 g/cm^3) used in model shown within model bodies. Lowest body in model has a density contrast of 0.00 g/cm^3 (effective density of 2.67 g/cm^3). Symbols: 1-well that penetrated Franciscan rock; 2-well that bottomed in Cenozoic deposits.

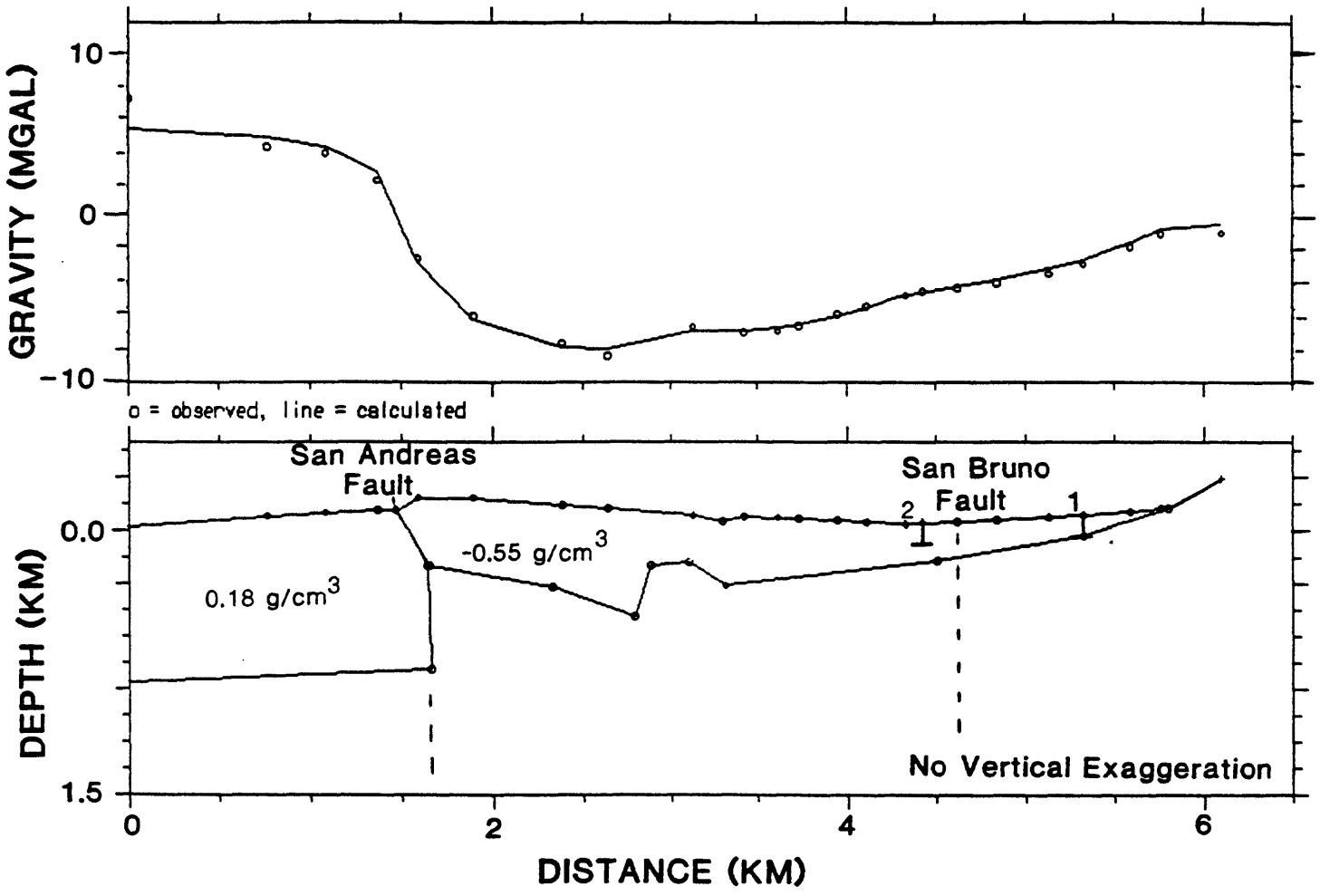
GRAVITY (MGAL)
10
0
-10
o = observed, line = calculated
San Andreas Fault
San Bruno Fault
2
1
-0.55 g/cm3
0.18 g/cm3
DEPTH (KM)
0.0
1.5
No Vertical Exaggeration
0
2
4
6
DISTANCE (KM)

Figure A-5a

Figure A-5b. Measured gravity along profiles g1-g5 (see figure A-2 for locations) registered to the San Bruno fault. Lower panel shows the theoretical gravity anomaly produced by a step in the surface of Franciscan rock 60 m high, and aligned beneath the San Bruno fault.

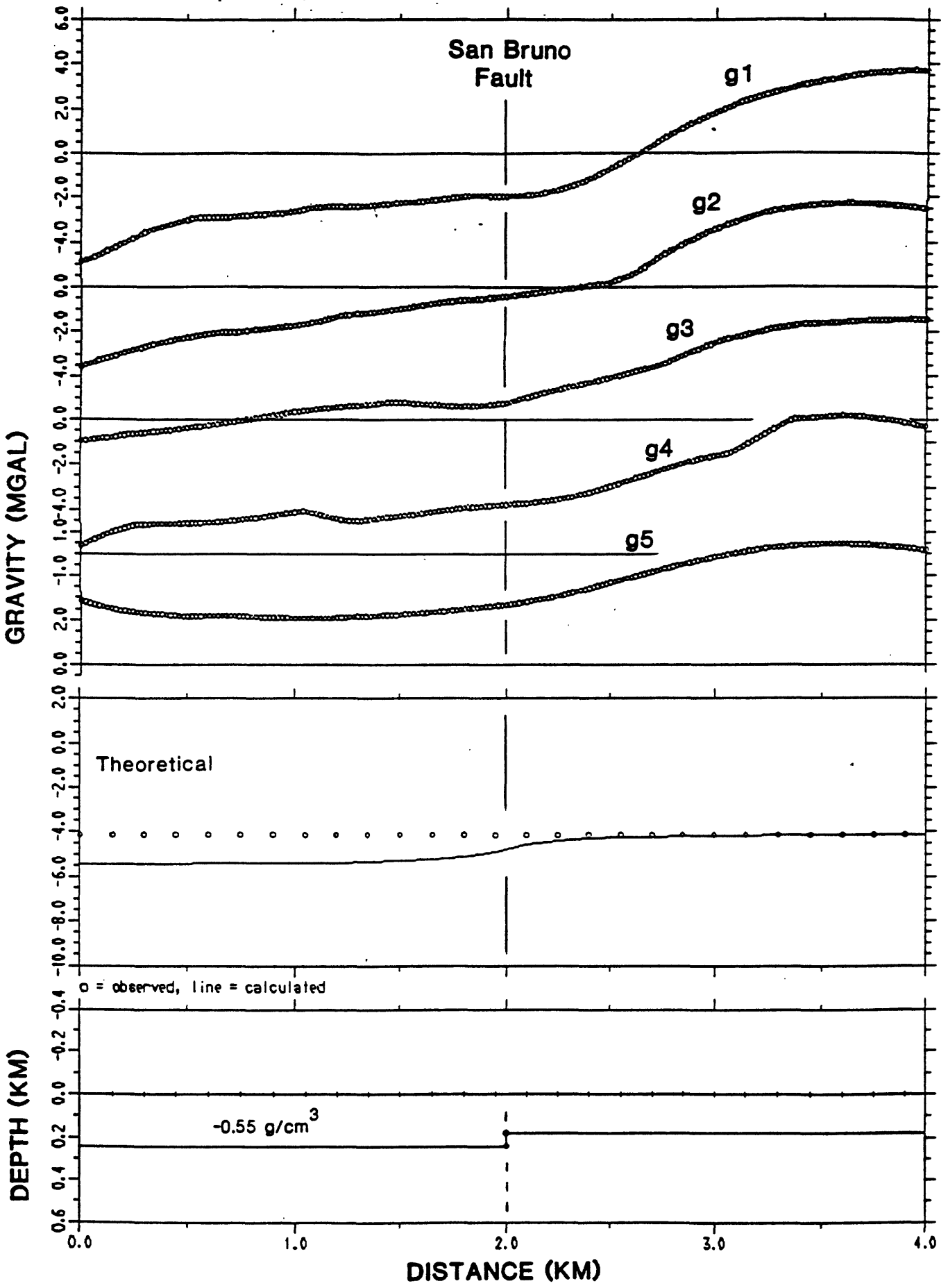
San Bruno
Fault
g1
g2
g3
g4
g5
GRAVITY (MGAL)
Theoretical
o = observed, line = calculated
DEPTH (KM)
-0.55 g/cm3
DISTANCE (KM)

Figure A-5b

B. DIGITAL GEOMORPHIC INVESTIGATION

by
A. S. Jayko

INTRODUCTION

Digital geomorphic investigations were requested by Bay Area Rapid Transit (BART) in May, 1996 to evaluate the location and existence of the San Bruno fault as inferred by Lawson (1914) and Bonilla (1971) in the vicinity of the proposed extension of BART from Colma to the San Francisco International Airport. The inferred San Bruno fault is loosely portrayed as having early Quaternary activity in a recent map compilation of faults in California (Jennings, 1994).

This study utilizes topographic data as recorded by the U.S. Coast Survey during the 1852-1869 interval, prior to extensive modification of the land surface by cultural development that is inherent in modern surveys since the turn of the century. The U.S. Coast Survey data set consists of four maps at 1:10,000 scale with 20-ft contour intervals. The focus of the investigation is to determine if there is geomorphic evidence for Quaternary activity along the inferred map trace of the San Bruno fault that can be enhanced by digital geomorphic analysis of the high resolution and less modified topography surveyed last century. The digital geomorphic analysis includes preparation of slope, curvature, and shaded relief maps as well as of surface profiles and drainage networks.

BACKGROUND

The land surface morphology is a recorder of a variety of natural and anthropogenic processes that include recent tectonic activities such as faulting and folding. Topographic lineaments including ridge, stream, saddle, slope break and depression alignments can form as the result of recent tectonic displacements. Likewise, stream diversions and knickpoints or convexity in stream profiles can be indicative of fault or fold activity. Digital geomorphic analysis provides a tool for rapid quantification of surface parameters as well as image enhancement of edge features derived from digital elevation models (DEM's). Geomorphic lineaments developed on the surface overlying the late Pleistocene Colma Formation that are not demonstrably fluvial in origin or due to pre-existing underlying bedrock structure can be interpreted as candidates for potentially active late Quaternary faults.

Four distinctive northwest trending geomorphic domains that are characterized by the remnants of perched erosional surfaces and locally by late Pleistocene marine terrace deposits occur in the study area (Smith, 1960): 1) an upland surface west of the San Andreas fault, the Sawyer surface, that ranges in elevation from 300 to 360 m is inferred to have underlain the Pliocene (?) to Pleistocene Merced Formation; 2) an upland, compound erosional surface east of the San Andreas fault, the Buri Buri surface that ranges in elevation from 180 to 250 m and which may have underlain late Pleistocene terrace deposits (Lawson, 1893) and Colma Formation (Bonilla, 1971); 3) the Colma surface which lies in a depression that crests at an elevation of about 60 m and extends to sea level with a drainage divide that separates Colma Creek, draining into San Francisco Bay, from the Lake Merced basin which drains into the Pacific; and 4.) San Bruno Mountain which is mainly an erosionally controlled feature that also has a remnant erosional upland surface and Quaternary (possibly dune sand) deposits locally preserved on it's northeast flank (Smith, 1960; Bonilla,

1971). These geomorphic features provide part of the important age control that establishes the geologic youthfulness of the land surface as well as the location and relative magnitude of the vertical displacements of crustal blocks in the study area.

The inferred trace of the San Bruno Fault (SBF) lies approximately 3.5 to 4.0 km northeast of the San Andreas fault zone, which is a well-known structure and the most active strike-slip fault in northern California (fig. B-1). Middle Pliocene (~3.0 Ma) and Pleistocene strata that lie east of the San Andreas are commonly inclined 40 to 80 degrees underlying the Buri Buri surface within two kilometers of the SBF. The SBF trace crosses late Pleistocene Colma Formation which is inferred to be about 127,000 to 73,000 years old (not younger than oxygen isotope stage 5) by Hunter and others (1984). The Colma Formation and younger alluvium are overlain by a weakly dissected very low-sloping erosional surface. Both the Sawyer surface and San Bruno Mountain are primarily underlain by indurated Mesozoic rocks of the Franciscan assemblage.

DATA

Four U.S. Coast Survey topographic maps (1:10,000 scale, 20 ft contour interval) of the San Francisco Peninsula produced between 1852 and 1867 were hand-traced, raster scanned, vectorized, edited, and attributed (Wentworth and others, unpub. data, 1996), and then gridded at 15 meter intervals to produce the digital elevation model used in this study (fig. B-2). A 15 m grid of elevations was created from a merged version of the four vectorized contour map sheets using the topographic gridding tool in the commercial GIS ARC/INFO (Environmental Systems Research Institute, Inc.). This TOPOGRID command uses an iterative finite difference interpolation technique that is optimal for generating hydrologically correct digital elevation models by imposing constraints that result in a connected drainage structure.

The resulting elevation grid was used to generate slope and curvature maps, as well as to make selected topographic profiles using functions in the ARC/INFO grid environment. The rate of elevation change per unit distance, the slope, is the first horizontal derivative of the elevation model. It is particularly useful for imaging and digitally selecting inclined or warped surfaces that may have a wide range in elevation values but a narrow range in slopes. The rate of slope change, the curvature, is the second horizontal derivative of the elevation. Curvature is particularly useful for imaging escarpments of various origins in the landscape. Oblique surface views and shaded relief maps provide useful images that illustrate continuity of morphologic features, variations in surface roughness properties and magnitudes of relief (figs. B-3 and B-4). The topographic profiles were made from the gridded elevation data.

DATA ANALYSIS

Derivative maps

Many prominent geomorphic features can be observed on the unmodified elevation contour map and DEM of the 1800s topography; thus they are useful on their own for lineament and surface analysis of potentially active tectonic structures (fig. B-2). The slope map enhances the surface continuity and the continuity of fluvial dissection across surfaces (fig. B-5). Slopes in the study area range from 0° to 68° with the steepest topography developed in the sea cliffs along the coast, the upper flanks of San Bruno Mountain and drainages that dissect the Buri Buri surface east of the San Andreas fault. Curvature values primarily range from -5 to 5 with negative values indicating upwardly concave surfaces (e.g., streams) and positive values indicating upwardly convex surfaces (e.g., ridges and slope breaks) (fig. B-6).

Topographic profiles and Drainage network
Topographic profiles oriented approximately normal to the structural and topographic grain of the study area were constructed at approximately 1.5 km intervals across the study area from Lake Merced to South San Francisco using the 15 m 1800s DEM's (figs. B-7 and B-8) and across San Bruno Mountain using the modern 30 m DEM's (figs. B-9 and 10). A set of profiles that show greater resolution of the Colma surface near the mapped trace of the San Bruno fault were also constructed at selected sites along the inferred map trace (figs. B-11 and B-12).

A drainage network was produced from the 1800s elevation grid using standard functions for hydrologic analysis which utilize flow direction combined with accumulation of flow to define a stream network. The accumulation of flow is determined by the cumulative number of uphill cells that flow into a given cell. The detail of the stream network in the upper reaches of the drainages is controlled by selecting for grid cells with smaller amounts of accumulated flow. The stream order, a method for identifying streams based on their number of tributaries, can be determined using either Strahler or Shreve counting methods, making possible the selection of higher order streams for digital analysis. For this study the minimum flow accumulation cell size was set at 25, the Strahler stream order assignment was used, and stream orders 3 and greater define the digitally generated drainage network (fig. B-13).

INTERPRETATION

Slope and Curvature maps
The northeast side of Colma Valley, where the trace of the SBF has been inferred, lacks any significant continuous lineaments that parallel the fault trace on either the slope or curvature grid maps (figs. B-5 and B-6), with the possible exception of the short, approximately 2 km long northeast shoreline of Lake Merced. Where the mapped trace of the SBF crosses Colma Creek, prominent topographic lineaments trend about 20° to the fault trace and do not noticeably terminate against it.

The low-slope surface on the southwest side of Colma Valley shows a strong continuous slope break which lies subparallel, but about 2 km east of the San Andreas (figs. B-2, B-5 and B-6) and trends about 320°. On the shaded relief map (fig. B-3) this break is seen to be irregular in detail. West of the Colma surface, in the Buri Buri upland area, prominent alignment of ridges and creeks 2 to 4 km in length trending approximately 135° are subparallel to the dominant strike of underlying Merced Formation strata (Bonilla, 1971) suggesting the ridge-creek lineament trend is structurally controlled and represents the bedding direction. These apparently strike parallel ridge-creek lineaments terminate near the edge of the Colma surface where the creeks change course to about 050° indicating a NE tilt direction approximately normal to the San Andreas fault.

Parts of Colma Creek, the headwaters of the Lake Merced basin, and the terrace edges that flank Lake Merced have weakly-developed, short straight stretches, 1-3 km in length that show on the slope and curvature maps (figs. B-5 and B-6). These stretches are subparallel to the trace of the SBF; however, they do not extend into adjacent areas of intact Colma surface, are irregular in detail as seen on the shaded relief map (fig. B-3), and are mainly located to the west of the trace of the fault and the area of the proposed BART extension.

The subparallel slope breaks on the southwest side of San Bruno Mountain, topographically above the mapped trace of the Hillside fault, tend to be subparallel to the bedding-parallel lineations of the

Buri Buri surface near the northwest extent of the San Andreas fault onshore (figs. B-2 and B-5) suggesting similar structural control on the orientation of these features.

Topographic profiles and Drainage network
Stacked topographic profiles (figs. B-7 and B-8) show the characteristic elevations and variations in surface roughness of the Buri Buri, Colma and San Bruno geomorphic domains. Topographic profiles showing the Colma surface that underlies the inferred fault trace (figs. B-11 and B-12) do not show systematic slope break or change in surface slope that might be indicative of late Quaternary activity. Drainages on the southwest slope of San Bruno Mountain and tributaries of Lake Merced do not show any noticeable lateral offset at the San Bruno fault trace at the scale of figure B-13. Profiles across San Bruno Mountain (figs. B- 9 and B-10) show asymmetric morphology with a steep southwest flank, a southwest tilted or facing surface, and flats preserved on the northeast flank, which if structurally controlled would indicate a buried, northeast dipping reverse fault at depth.

Drainages west of the axis of the Colma depression, which incise the west side of the Colma surface, dominantly trend normal to the San Andreas fault zone and the Buri Buri surface (figs. B-2 and B-13). The drainages on the east side of the Colma depression tend to have a more radial (elliptical) pattern with respect to San Bruno Mountain suggesting different origins to the range fronts of the respective highs (fig. B-13).

CONCLUSIONS

Derivative maps produced by digital processing of detailed topographic surveys where the San Bruno fault has been inferred to underlie Quaternary deposits lack any linear features that would be suggestive of post Colma Formation displacement underlying the proposed extension of the BART alignment between Colma and the San Francisco International Airport. Structurally and stratigraphically controlled linear features developed on geologically youthful (late Pleistocene) erosional surfaces with continuity of 2-4 km, and more rarely up to 15-20 km are present elsewhere in the study area, indicating that the methodology can delimit such features.

There is no digital geomorphic evidence that can be ascertained from 1800s U.S. Coast Survey-derived 15 m elevation data for the existence of the San Bruno fault where the fault trace is currently inferred. If the topography of San Bruno Mountain were actually controlled by a Quaternary fault, then the geomorphology suggests that such a fault would be a northeast dipping, southwest-verging blind reverse or thrust fault. This possibility is suggested by: 1) an asymmetric topographic high with a steep southwest flank and more gentle northeast flank, and perched erosional upland and associated Quaternary (possibly dune) sand deposits (Bonilla, per. com., 1996) on the northeast flank of the mountain; 2) southwest facing convexity of the lower slope edge of San Bruno Mountain; and 3) radially or elliptically developed drainage away from the southwest flank of the mountain. Bedding orientations within the Franciscan complex that underlies San Bruno Mountain (Bonilla, 1971) are consistent with a southwest verging anticline in the hanging-wall of such a fault. The absence of a geophysical anomaly (Jachens, this report, Part A), however, requires that such a structure be blind (that is, not reaching the ground surface), with a tip-line deeper than 1.5 to 2 km, below the base of the Merced Formation.

Figure B-1. Shaded Relief Map from modern 30 m digital elevation model (DEM) showing, inside white line, location of digitized 1800s U. S. Coast Survey topography .

Shaded Relief Map from modern USGS 30m DEM

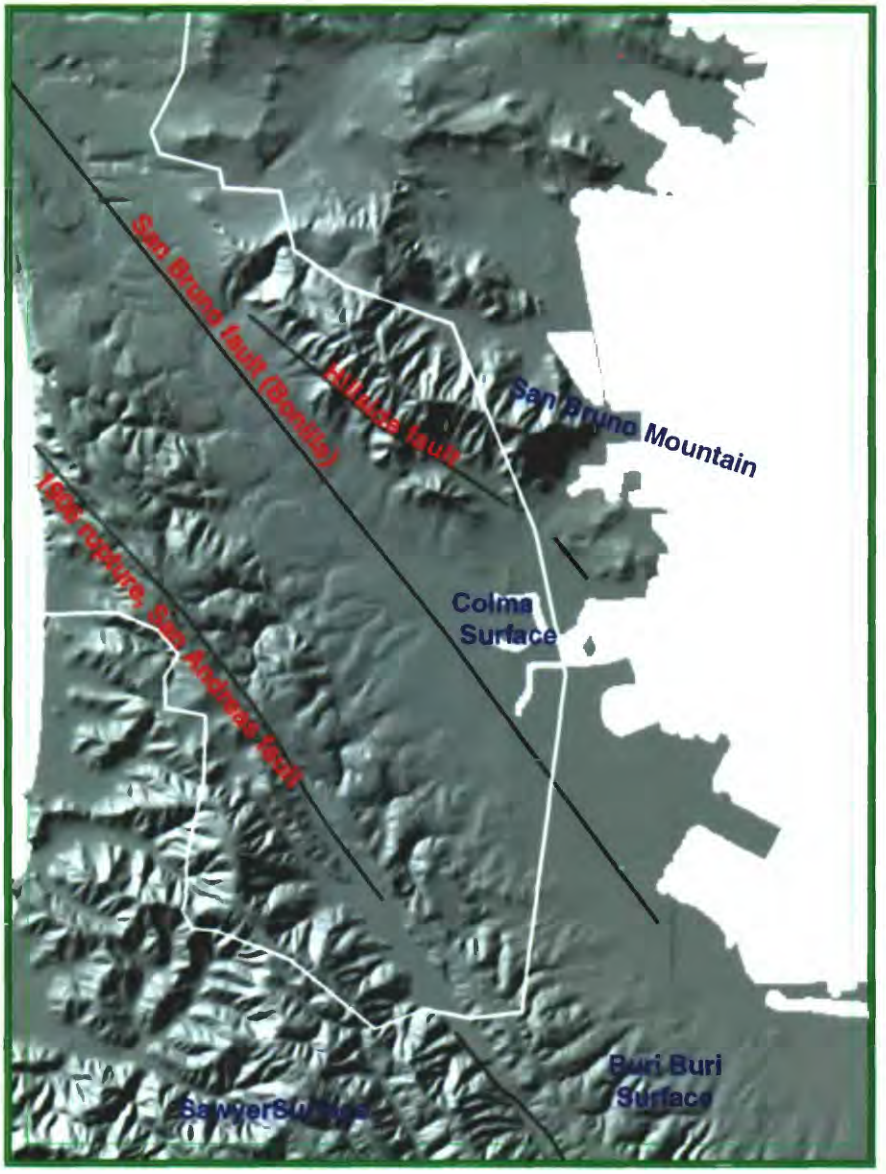

SCALE 1:125000

1 .5 0 1 2 3 4 5 6 7 MILES

1 .5 0 1 2 3 4 5 6 7 KILOMETERS

0 2 4 6 8 10 12 14 THOUSAND FEET

Figure B-1

Figure B-2. Map showing the digitized vector contours of the 1800s U. S. Coast Survey topography (modified from Wentworth and others, unpub. data, 1996).

Contour map of 1800s USGS topography

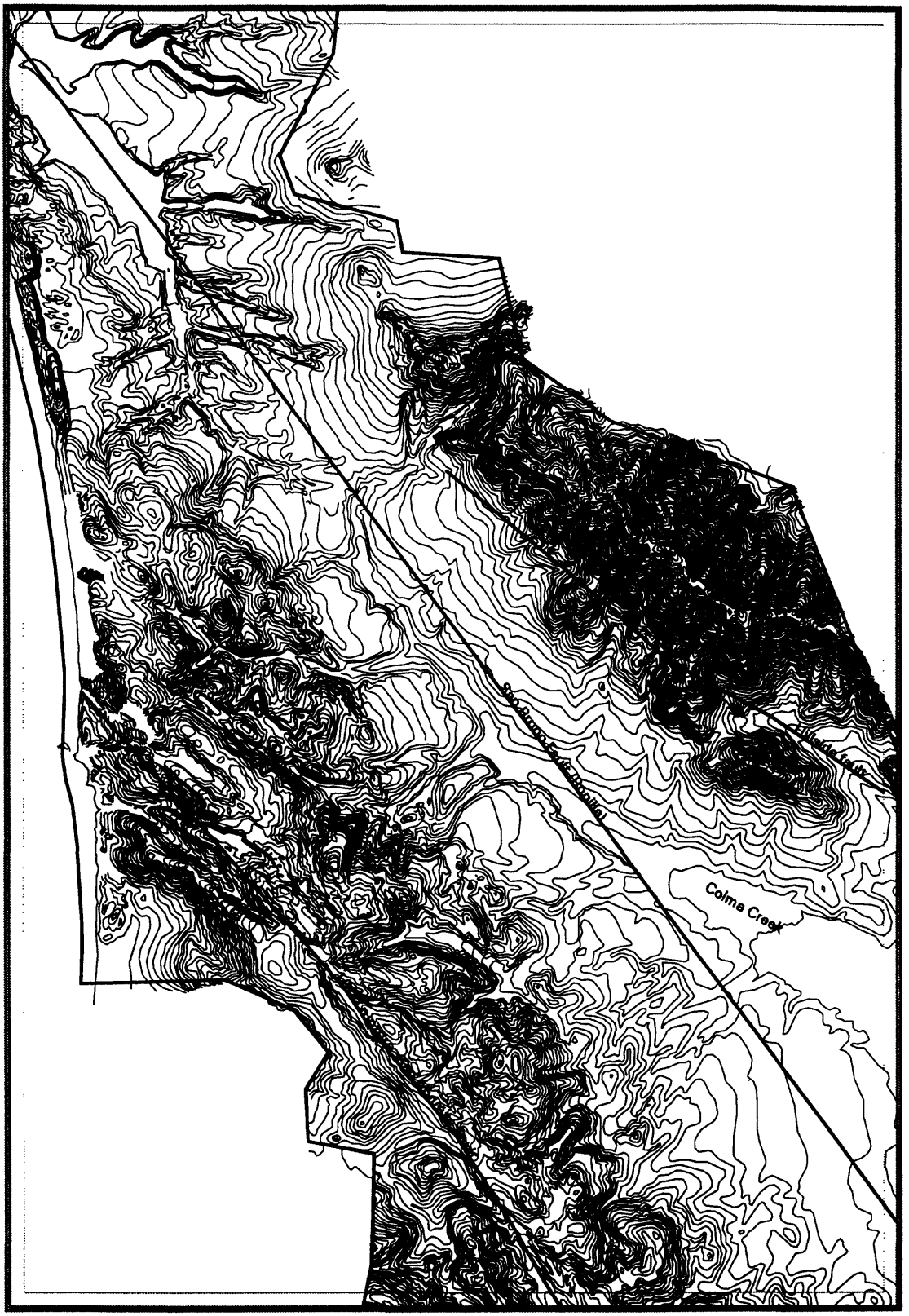

SCALE 1:60000

Figure B-2

1 .5 0 1 2 3 4 5 MILES

1 .5 0 1 2 3 4 5 KILOMETERS

0 1 2 3 4 5 6 7 8 9 10 11 THOUSAND FEET

Figure B-3. Shaded relief map made from 1800s 15 m elevation grid.

Shaded Relief Map, 1800s grid

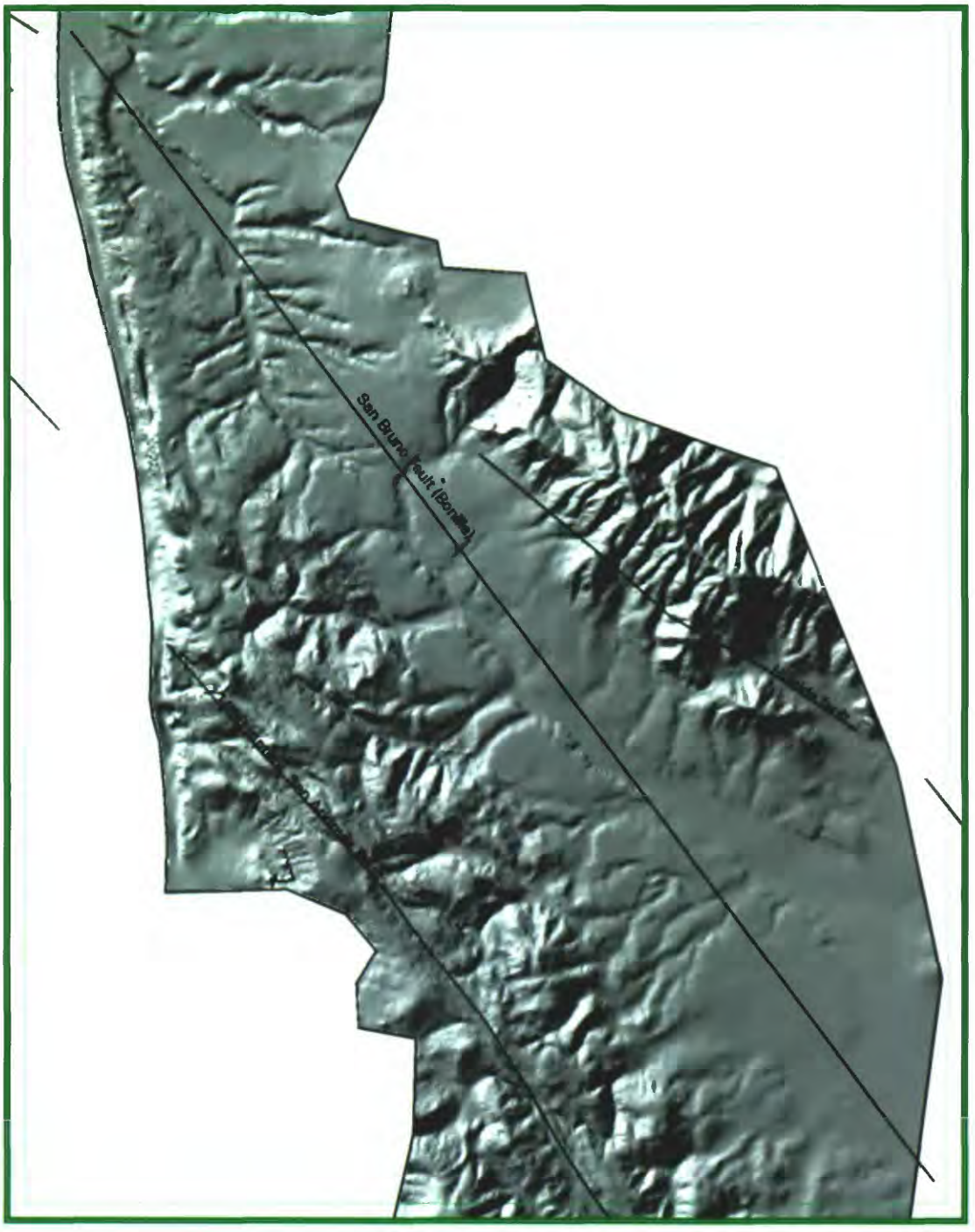

SCALE 1:75000

1 .5 0 1 2 3 4 5 MILES

1 .5 0 1 2 3 4 5 KILOMETERS

0 1 2 3 4 5 6 7 8 9 10 11 THOUSAND FEET

Figure B-3

Figure B-4. Oblique surface view with draped shaded relief image. Looking from northwest to southeast down the axis of the Colma depression.

Oblique view, 1800s digital topography

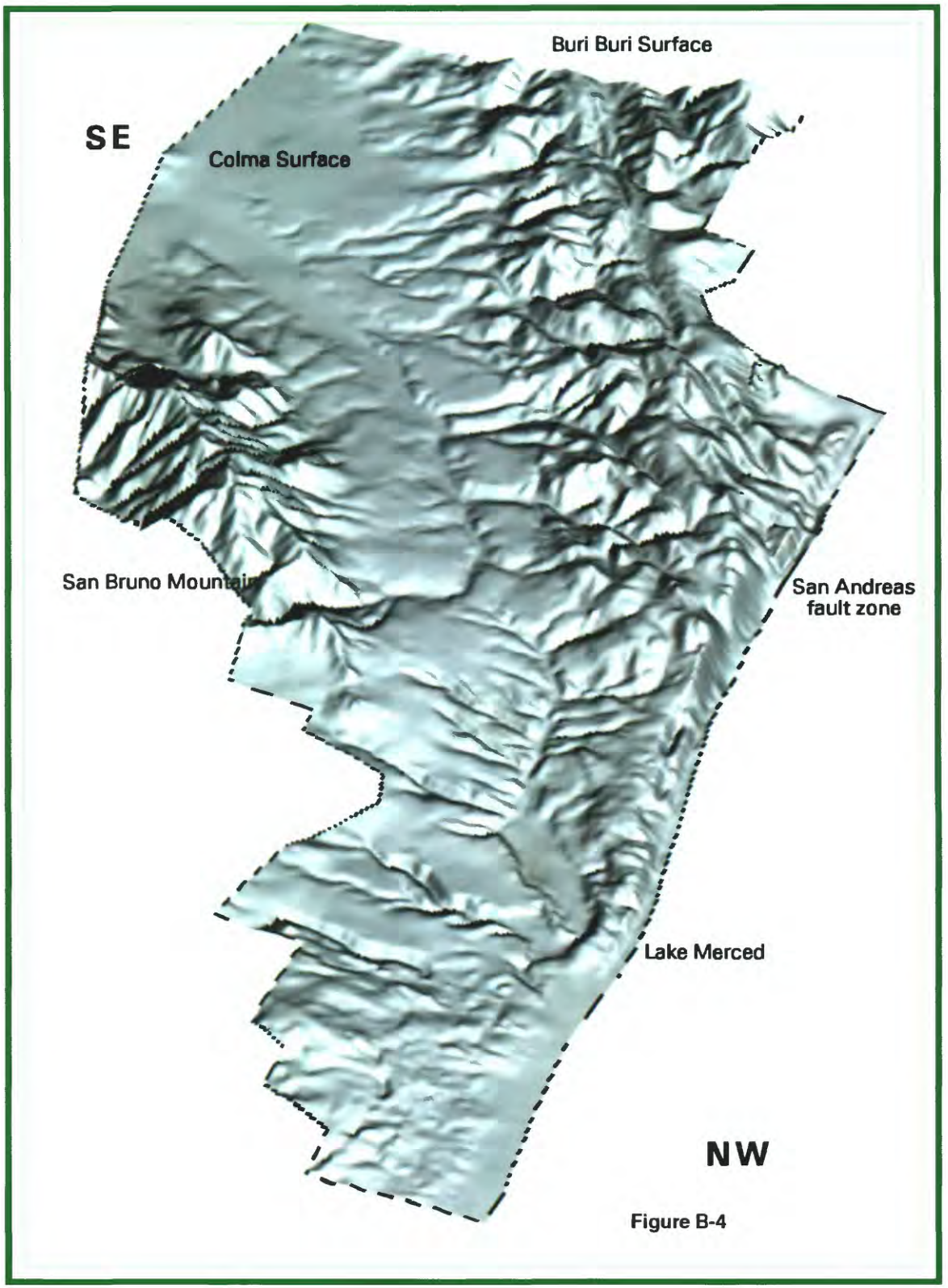

Figure B-4

Figure B-5. Slope map (low slopes dark, high slopes light) from 1800s grid.

Slope Map, 1800s grid

SCALE 1:75000

1 .5 0 1 2 3 4 5 MILES

1 .5 0 1 2 3 4 5 KILOMETERS

0 1 2 3 4 5 6 7 8 9 10 11 THOUSAND FEET

Figure B-5

Figure B-6. Slope curvature map from 1800s grid. In general, streams concave-upward are dark, ridges or slope edges convex-upward are light.

Curvature Map (2nd derivative), 1800s grid

SCALE 1:75000

1 .5 0 1 2 3 4 5 MILES

1 .5 0 1 2 3 4 5 KILOMETERS

0 1 2 3 4 5 6 7 8 9 10 11 THOUSAND FEET

Figure B-6

Figure B-7. Map showing location of topographic profiles for Figure B-8, elevation grid with 25 m contours.

Location of Topographic profiles, 1800s DEM

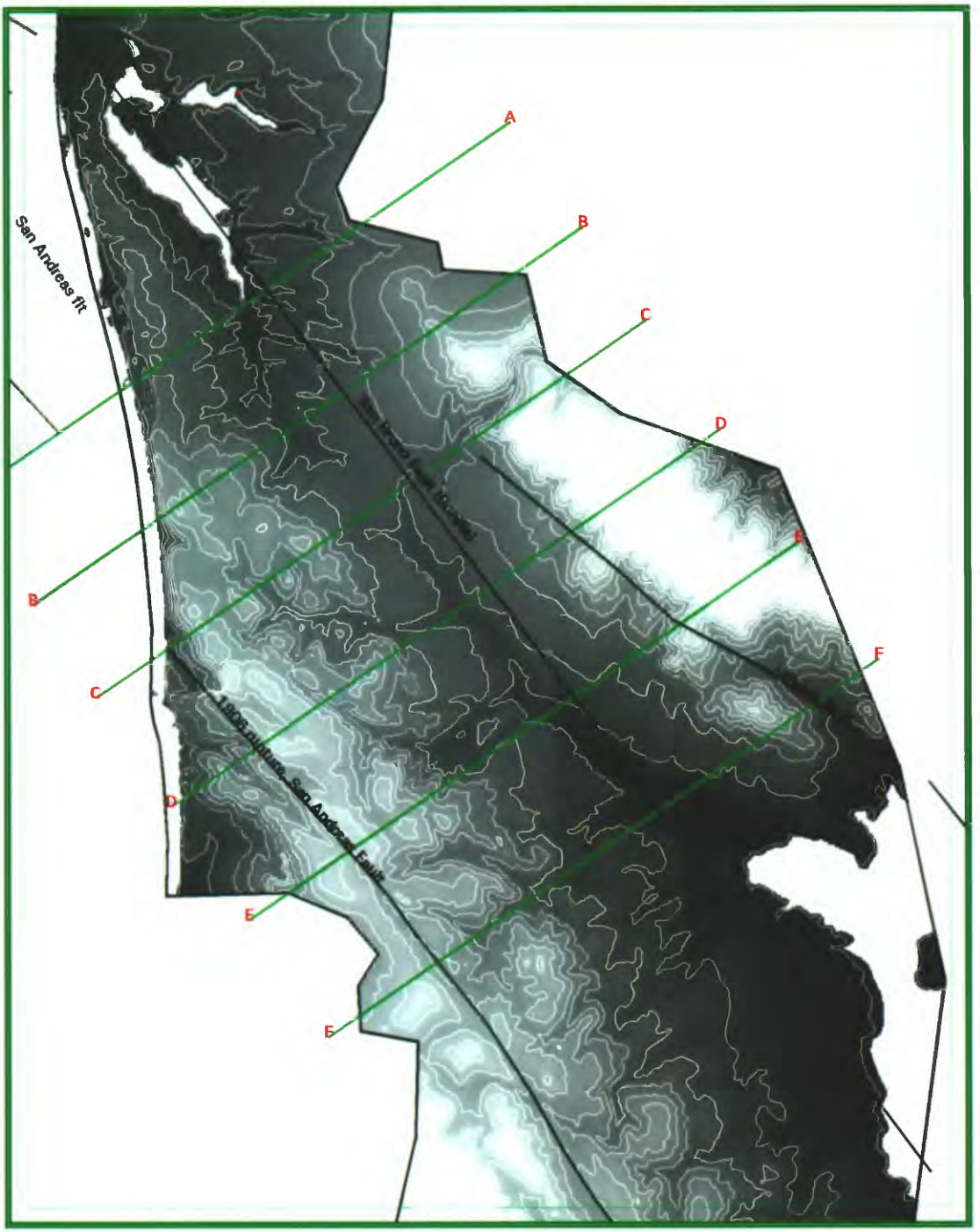

SCALE 1:75000

1 .5 0 1 2 3 4 5 MILES

1 .5 0 1 2 3 4 5 KILOMETERS

0 1 2 3 4 5 6 7 8 9 10 11 THOUSAND FEET

Figure B-7

Figure B-8. Stacked topographic profiles A-F, 1800s topography. Horizontal and vertical scales in meters.

Figure B-8

Topographic Profiles, 1800s Topography, normal to SAF

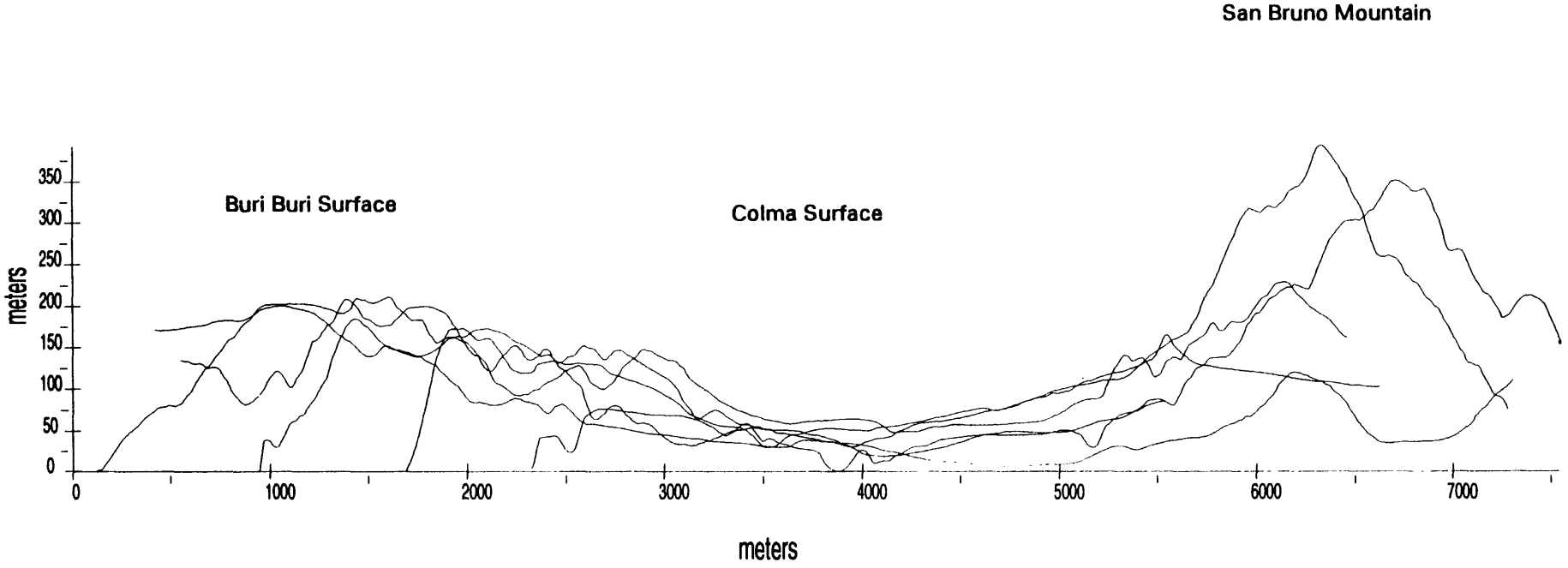

Figure B-9. Location of modern topographic profiles, San Bruno Mountain.

Topographic profiles, San Bruno Mountain, modern DEMs

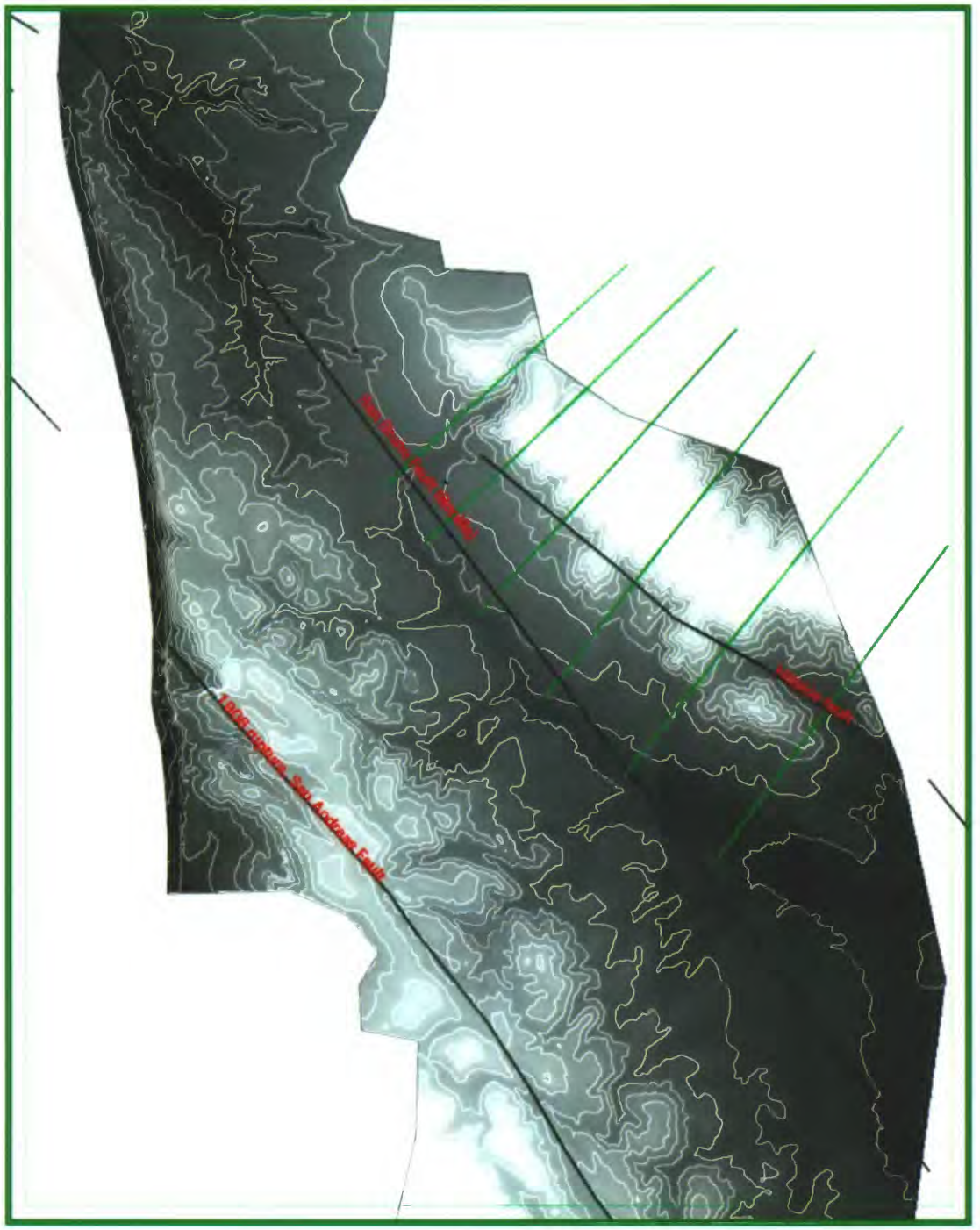

SCALE 1:75000

1 .5 0 1 2 3 4 5 MILES

1 .5 0 1 2 3 4 5 KILOMETERS

0 1 2 3 4 5 6 7 8 9 10 11 THOUSAND FEET

Figure B-9

Figure B-10. Topographic profiles, San Bruno Mountain, from modern 30 m elevation grid.

Figure B-10

Modern Topography, 30 m, San Bruno Mountain

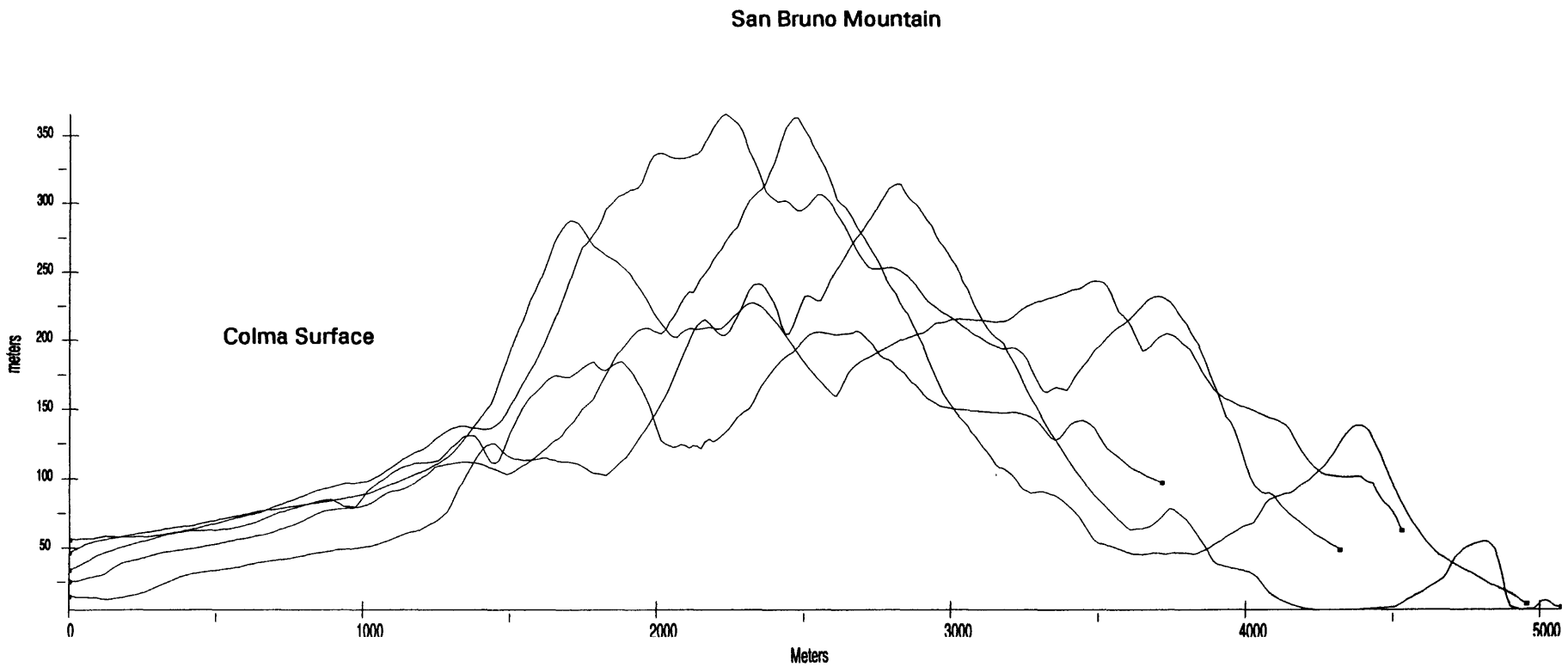

Figure B-11. Map showing location of topographic profiles A-G from 1800s digital elevation model (DEM) crossing inferred trace of San Bruno fault.

Location of Topographic profiles, San Bruno Fault, 1800s DEM

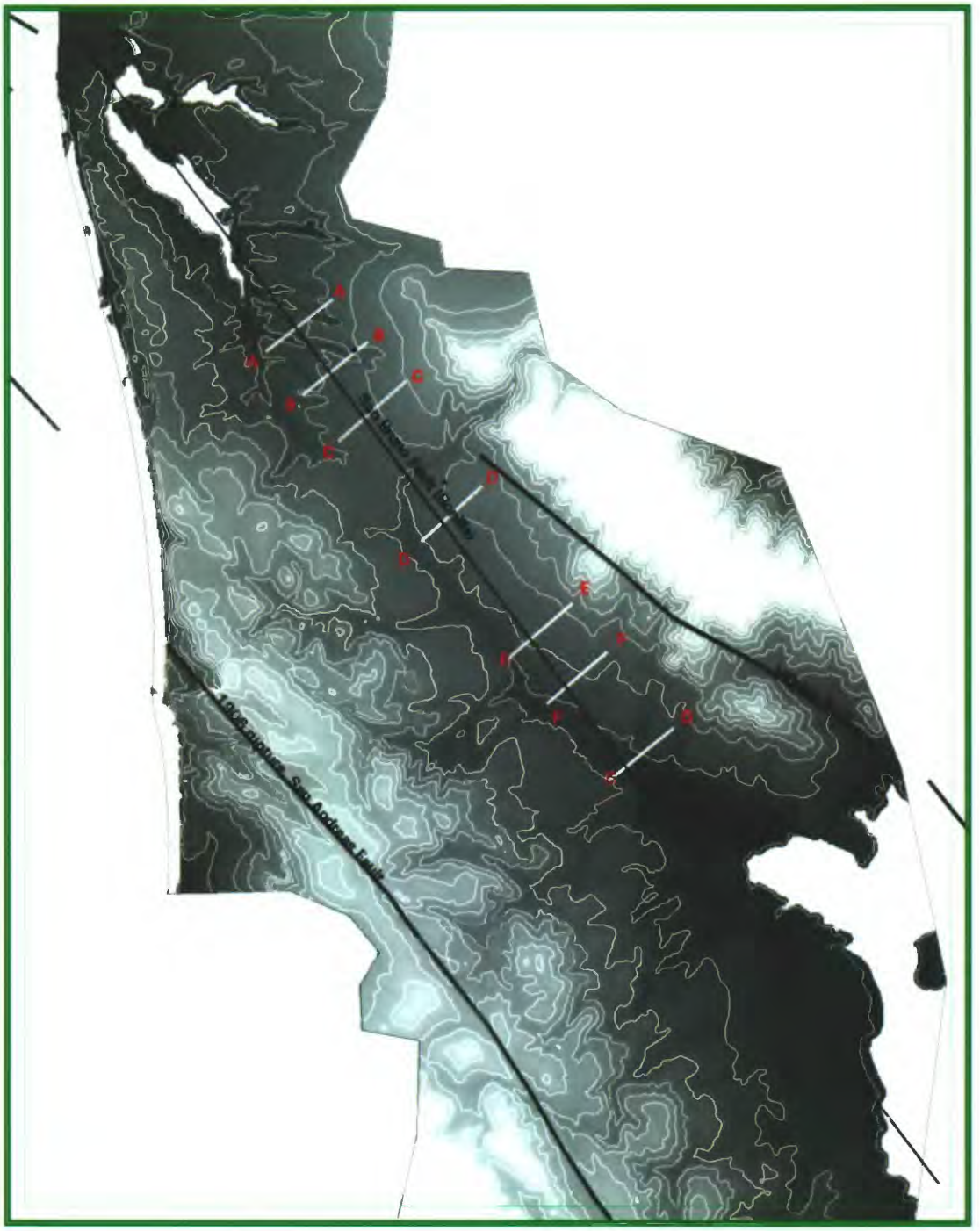

SCALE 1:75000

1 .5 0 1 2 3 4 5 MILES

1 .5 0 1 2 3 4 5 KILOMETERS

0 1 2 3 4 5 6 7 8 9 10 11 THOUSAND FEET

Figure B-11

Figure B-12. Topographic profiles A-G from 1800s digital elevation model, crossing inferred trace of San Bruno Fault.

Topographic Profiles, San Bruno Fault

Figure B-12

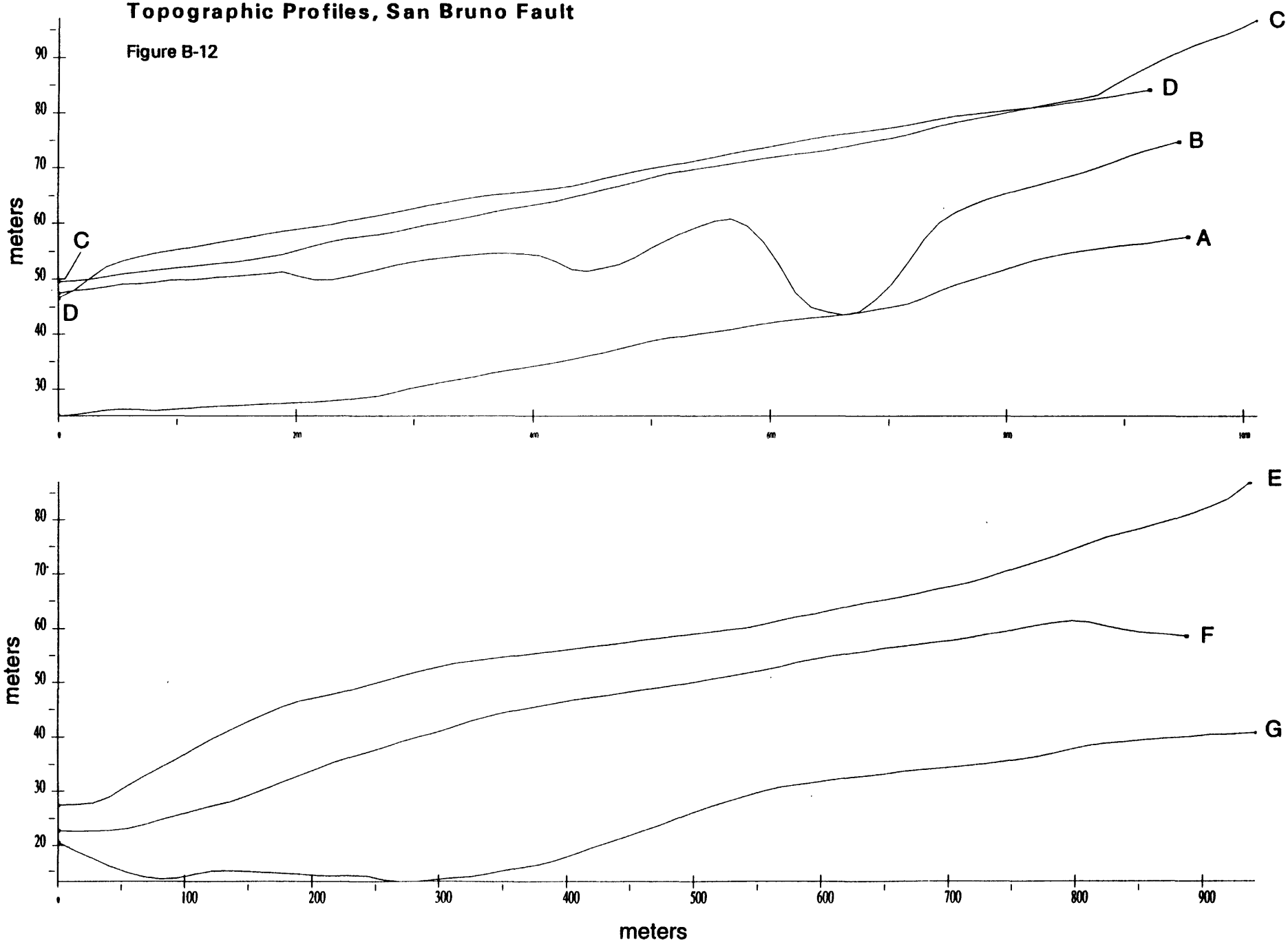

Figure B-13. Map showing drainage network generated from flow direction and flow accumulation functions using 1800s elevation grid.

Drainage network

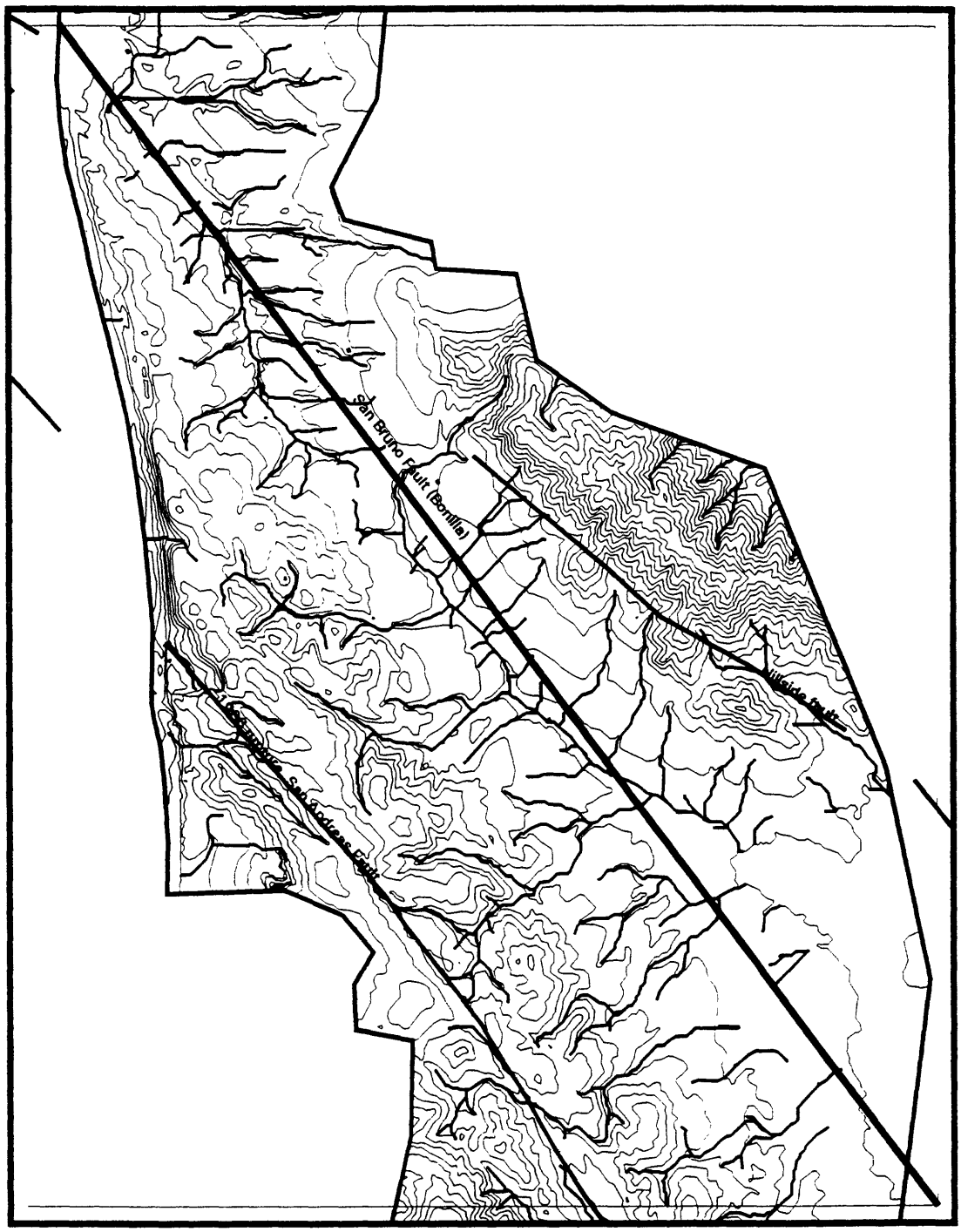

Figure B-13

C. ANALYSIS OF SUBSURFACE DATA

by
M.G. Bonilla

INTRODUCTION

This investigation is based on logs of borings supplied by BART, supplemented by logs of borings and unpublished geological information in USGS files. The general setting, place names, and principal faults are shown on figure A-1.

GEOLOGIC SETTING

Geologic units
A simplified geologic map (fig. C-1) shows the principal geologic units in the area studied. A brief description of the distribution and pertinent characteristics of these units follows.

The oldest unit is Franciscan bedrock, exposed at the surface to the northeast of and extending below the other geologic units. The bedrock has been penetrated in several borings in the northeast and southeast part of the study area, but is deeply buried in the southwest and northwest parts. The Merced Formation, of Pliocene (?) and Pleistocene age, crops out to the southwest and overlies the Franciscan bedrock at an uncertain depth beneath the study area. The Pleistocene Colma Formation overlies the Merced Formation and extends to the ground surface over most of the study area. The age of the Colma Formation is not well known. It has been estimated to be on the order of 100,000 years (Clifton and Hunter, 1987), but some of it may be younger—a borehole sample gave a radiocarbon age of about 34,000 years (Caldwell-Gonzalez-Kennedy-Tudor, 1982A; J.R. Powell, 1993, personal communication). A radiocarbon age of 10,540±250 years (Rubin and Alexander, 1960, p. 155) from a stream terrace younger than the Colma Formation shows that the Colma is older than 10,000 years.

Occupying channels cut into the Merced and Colma Formations is Quaternary alluvium, some of which is of early Holocene age but most of which is of late Holocene age. Holocene Bay mud interfingers with the alluvium in the southeast part of the area. Artificial fill covers the Bay mud and parts of various other geologic units.

The geologic units above the Franciscan bedrock have a low density relative to the Franciscan bedrock, and are unconsolidated except for thin locally cemented beds in the Merced and Colma Formations.

Geologic structure
The San Andreas and Serra faults, and the Hillside fault, which lie to southwest and northeast of the study area, are not of direct interest to this investigation and will not be discussed.

The San Bruno fault was postulated by Lawson (1895, 1914) as forming the boundary between the Franciscan bedrock of San Bruno Mountain and the soft rocks of the Merced Formation to the west, and therefore he mapped the fault close to the base of San Bruno Mountain. On the basis of borehole records that showed bedrock in the subsurface extending west of Lawson's fault line and

a gravity survey by Greve (1962), Bonilla (1964, 1965, and 1971) placed the fault westward of all known occurrences of bedrock in the vicinity, but labeled the fault as hypothetical on all three maps.

Several relatively recent investigations bear upon the age, location, and existence of the San Bruno fault. Offshore geophysical surveys have detected a zone of faults that are approximately in line with the San Bruno fault as postulated onshore. A map of this offshore zone, by McCulloch and Greene (1990), indicates the zone as "active or potentially active." This phrase is not defined on the map but a companion report (Kennedy and others, 1987) states that such features are considered to be "potential geologic hazards," and the examples given show offset of sedimentary deposits of late Pliocene to Quaternary age. Because the term "Quaternary" includes modern times, this implies that the displacement could be very young.

Epicenters of small earthquakes shown on recent maps suggest modern activity on the offshore fault zone and its onshore projection. One map (Cockerham and others, 1990) shows earthquakes that occurred in the period 1926-1986, and the others cover the period 1969-1994 (Zoback and Olson, 1994; Zoback and others, 1995). These maps show epicenters near the offshore fault zone and its onshore projection. More recent studies suggest that the San Andreas fault steps eastward toward Lake Merced, and that the offshore zone may actually be part of the San Andreas fault itself (Jachens and others, 1996; Zoback and Jachens, 1996).

At three onshore locations, faults that may be part of the San Bruno fault apparently affect the Colma Formation. Hengesh and Wakabayashi (1994, 1995) have identified a fault that they believe displaces the Merced Formation and apparently has tilted the lower part of the Colma Formation. This fault trends northwest-southeast and is in line with the onshore projection of the offshore fault zone discussed in the preceding two paragraphs. A probable fault inferred from tunnel information may have displaced the Colma Formation (Bonilla, 1994). The orientation of this probable fault is unknown, but its position is also in line with the onshore projection of the offshore fault zone . A Mini-Sosie seismic reflection survey at a proposed tunnel line found a structural discontinuity that has been interpreted as a fault displacing the Colma Formation (Caldwell-Gonzalez-Kennedy-Tudor, 1982B, p. 19-20). The drill hole nearest the discontinuity (Caldwell-Gonzalez-Kennedy-Tudor, 1982C, Boring 2-38) shows 75 ft of clay and sandy clay which the log labels as part of the Colma formation, but it may be in the Merced Formation (Yates and others, 1990, section B-B' do put the clay in the Merced fm). The discontinuity, marked as a heavy black line on the seismic profile (Caldwell-Gonzalez-Kennedy-Tudor, 1982D, app. C), is not shown above a depth of about 400 ft, well below Boring 2-38; thus the discontinuity may all be in the Merced Formation.

THE SUBSURFACE DATA

Borings

Many borings are available for the area of interest. All of the borings have descriptions of the material penetrated but, because most of them are water wells or shallow holes for housing developments, few have detailed geotechnical information. The borings made for BART (Geotechnical Consultants, Inc., 1995) were the most useful, containing detailed descriptions, blow counts, grain size analyses, and Atterberg limits. More comments about borings are made below in the descriptions of the geologic cross sections.

Cone Penetration Tests

Cone penetration test (CPT) results are available along the BART alignment. They include measurements of pore pressure as well as cone tip resistance and local friction. The CPT data supplement the borings and are very valuable in making correlations of sedimentary layers and geologic formations. The use of the CPTs is described below in the discussion of cross section A-A'.

THE CROSS SECTIONS

Three cross sections (locations shown on fig. C-1) were prepared, two perpendicular to the San Bruno fault and one nearly parallel to it. A northwest-southeast section (A-A,' fig. C-3A) covers 13,000 ft of the BART alignment. It is at a poor angle to evaluate the fault but includes by far the best and most comprehensive data. Two east-west cross sections, B-B' and C-C' (figs. C-4 and C-5) are nearly at right angles to the San Bruno fault, but the subsurface data are generally sparse, and have little geotechnical information.

Points on lithologic layers and formation boundaries are drawn as straight lines between data points to minimize interpretation, even though the resulting sections look unrealistic. For example, the buried alluvium-filled valley at 5200 ft on the horizontal scale of section A-A' (figs. C-3A, C-3B) is not likely to have its deepest part precisely at boring BRTSFO-29, nor likely to have a v-shaped cross-section.

The vertical exaggeration, indicated on each section, ranges from 10x to 67x. This exaggeration is necessary to include details without having very large illustrations, but the viewer must keep in mind that this greatly distorts the true dip of the layers and geologic contacts.

Lithologic correlations and identification of formation contacts were done without regard to the inferred position of the San Bruno fault. The lithologic symbols used in the cross sections are shown on Figure C-2.

Section A-A'

Section A-A' (figs. C-3A and C-3B) is at a poor angle to evaluate the San Bruno fault, but it includes the most abundant and best subsurface data. The BART investigation report (Geotechnical Consultants, Inc., 1995) includes borings spaced about 750 ft apart and CPTs generally half way between the borings. A few CPTs were at the same locations (within about 10 ft) of borings, which helped correlate information between CPTs and borings. The advice and active help of Michael J. Bennett of the USGS, who has much experience in relating CPTs to soil properties and in making correlations, materially improved section A-A.'

Correlation of lithologic units between the controls provided by borings and CPTs is based on various factors which were used to the extent that they were available and appropriate. Among the useful factors were lithologic descriptions, color, standard blow counts, CPT tip resistance and friction ratio, grain-size analyses, Atterberg limits, and recognition of fining-upward or fining-downward sequences (i.e., systematic variation in grain size) interpreted from the CPTs.

Drawing of contacts separating artificial fill, alluvium, and Colma Formation generally follows the picks shown on the BART logs and CPTs, but all of these previously interpreted picks were reexamined. At one locality which had both a boring (BRTSFO-25) and a CPT (no. 31), we moved a clay/sand contact within the alluvium on the basis of the CPT results, which were obtained after the boring was made.

The correlations between units shown on section A-A' are not a certainty, but represent our best judgment using the factors outlined above.

Section B-B'
Most of the borings used for section B-B' (fig. Figure C-4) are shallow holes drilled for housing developments in the 1950s and 1960s; the exceptions are two BART borings and one for a hospital. Generalized data from a water well was projected 390 ft into the section to infer the depth to the Franciscan bedrock. Other nearby borings as well as unpublished and published USGS near-surface geologic information were also used in preparing the section. Section A-A' clearly shows the lithologic variations that can occur in the Colma Formation in short distances, and that data from borings cannot be extended far from the position of individual borings; thus most of section B-B' is shown merely as the most common lithology in the Colma Formation in that area, silty sand. The interfingering relations of the slope debris (colluvium) with other unconsolidated sediments shown in the eastern part of the cross section is schematic.

Section C'-C'
The four deep borings on section C-C' (fig. C-5) are water wells, for which only general descriptions of the lithologic units and no formation names are available. The contact between the Colma and Merced Formations was inferred by Bonilla, mostly on the basis of the first occurrence of thick layers of blue clay, which are rare in the Colma Formation. The contacts between artificial fill, bay mud, and the Colma Formation are based on interpretation of information from four borings that lie at distances of 1100 to 1400 ft on either side of the section line.

No reliable basis was found for correlating the unconsolidated lithologic units between borings in this section. The variability over short distances of units within the Colma Formation is evident in section A-A.' Similar variations are known to occur within the Merced Formation. In excellent exposures of the Merced provided by cuts for housing developments and by seacliffs, only a few beds could be traced more than several hundred feet (Bonilla, unpublished data). In addition to variation in lithology, correlation of layers within the Merced in section C-C' is problematical because the dip, and variation in dip, are unknown. In surface exposures to the west, bedding in the Merced Formation dips 30-50° and strikes northeast to northwest (Bonilla, 1971).

The position of the surface of the Franciscan bedrock is based on the deep wells shown on the section supplemented by contours shown on the bedrock-surface maps of Bonilla (1964) and Hensolt and Brabb (1990). These maps are based on interpretation of borings in the vicinity and are moderately well controlled inasmuch as the bedrock has been reached by many borings to the southeast of the section. Although fault displacement of the bedrock surface cannot be ruled out, neither do the data suggest any displacement.

DISCUSSION

Despite the unfavorable angle that section A-A' makes with the trend of the San Bruno fault, it provides the best evidence regarding the fault. No single lithologic unit can be traced across the whole section, but particular lithologies or closely related lithologies form zones within the Colma Formation that overlap across almost the whole section. Most of these zones are clays or silts with admixtures of fine sand, lithologies that are difficult to separate during field logging and sometimes difficult to separate even with Atterberg limits tests. These variations in grain size probably represent facies changes within the zones, and were so interpreted in this study.

Considering that the fault intersects the section at a small angle, and assuming that the correlations are correct, this overlapping series seems to preclude the existence of a fault with a vertical separation of more than a few feet within the Colma Formation, except between BRTSFO-28 and CPT 36, the inferred location of the San Bruno fault (fig. 3B). At that location, a relatively clean sand near the bottom of BRTSFO-28 was not recognized in CPT-36; however, this sand did not extend westward to BRTSFO-27 either. Whether the silt near the bottom of BRTSFO-29 extends westward to BRTSF0-28 is unknown. Lithologic units within the alluvium shown on section A-A' also seem to preclude a fault, again with the possible exception of the interval between BRTSFO-28 and CPT 36.

The valley filled with alluvium shown at 5200 ft on the horizontal scale of section A-A' (fig. C-3A) is not related to the San Bruno fault, because it developed along Twelvemile Creek, nearly perpendicular to that fault. That lithologic zones within the Colma Formation cannot be matched across this alluviated valley is not unexpected in view of the horizontal variations visible in other parts of section A-A.'

Section B-B' (fig. C-4) provides no evidence for or against the existence of the San Bruno fault.

Section C-C' (fig. C-5) suggests that neither the Colma-Merced or the Merced-Franciscan contacts are vertically displaced by faulting but, in view of the uncertain correlations, vertical separations of several tens of feet could exist and not be recognized.

The change in character of the Colma Formation at Chestnut Avenue reported by Geotechnical Consultants, Inc. (1995, p. 15), which coincides with the position of the San Bruno fault as shown by Bonilla (1971) is reflected to some extent by cross section A-A' (fig C-3A). The fine-grained component of the Colma Formation at the ground surface increases, in general, to the southeast (Bonilla, 1959, p. 32; 1971, map explanation). Detailed examination, for this investigation, of unpublished data from surface exposures and borings shows that the surface and near-surface part of the Colma Formation in the area of figure 1 is predominantly silty or clean sand in the northwest and predominantly silt, clay, or clayey sand in the southeast, separated by a broad transitional zone. Thus, the change near Chestnut Avenue probably reflects sedimentary variation in the Colma Formation rather than faulting.

CONCLUSION

The subsurface and surface data do not suggest the existence of the San Bruno fault, but instead supply strong evidence that if the fault does exist, it has little or no effect on the Colma Formation or alluvium along the BART alignment in the area investigated.

Figure C-1. Simplified geologic map showing location of borings and cross sections. Labels of borings may differ from numbers used by Leighton and others (1995). Borings labelled BRTSFS-25, etc. are from Geotechnical Consultants, Inc. (1995). Geologic boundaries are from Bonilla (1971) modified using unpublished data. Surficial deposits less than 5 ft thick are not shown.

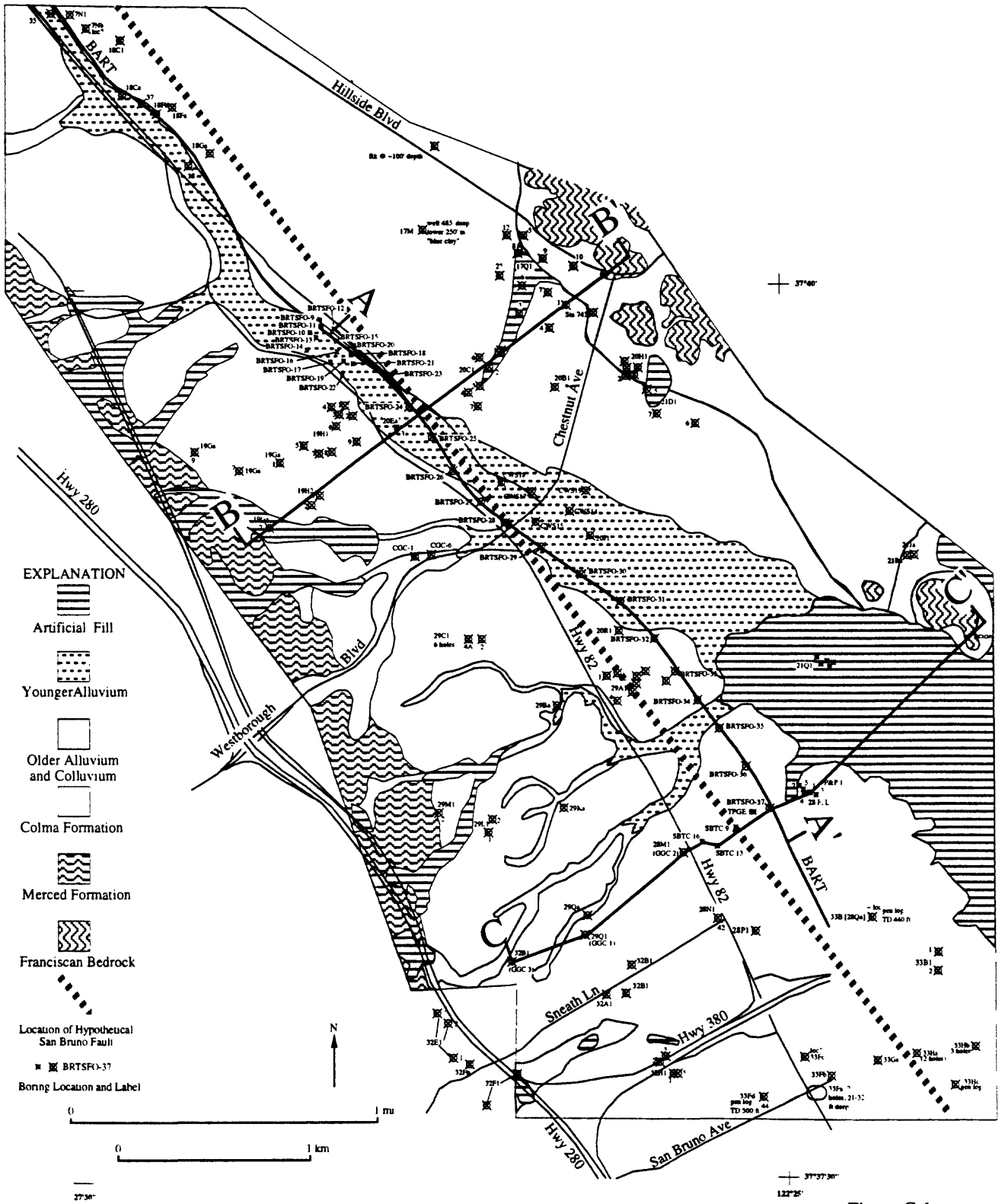
BART
Hillside Blvd
Chestnut Ave
Hwy 280
Westborough Blvd
Hwy 82
Sneath Ln
Hwy 380
San Bruno Ave
A
A'
B
B'
C
C'
EXPLANATION
Artificial Fill
YoungerAlluvium
Older Alluvium and Colluvium
Colma Formation
Merced Formation
Franciscan Bedrock
Location of Hypothetical San Bruno Fault
BRTSFO-37
Boring Location and Label
N
0
1 mi
0
1 km

Figure C-1

EXPLANATION FOR CROSS SECTIONS

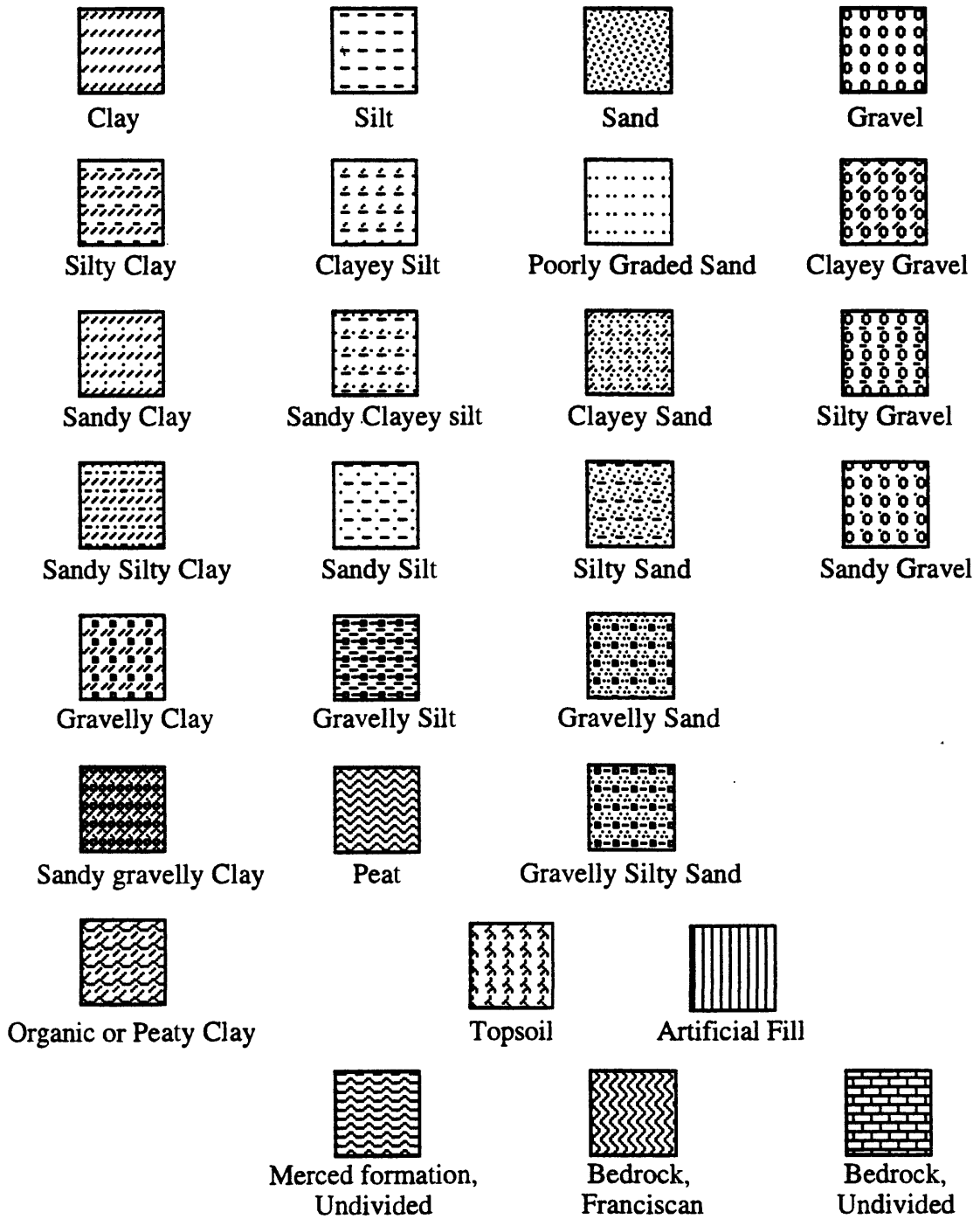

Figure C-2. Explanation of symbols used in figures C-3A, C-3B, C-4, and C-5.

Figure C-3A. Cross section A-A'. Section is parallel to BART alignment. Heavy lines separate artificial fill (at top), alluvium, and Colma Formation (at bottom). Vertical exaggeration 67x. CPTs above apparent ground surface are projected to section line.

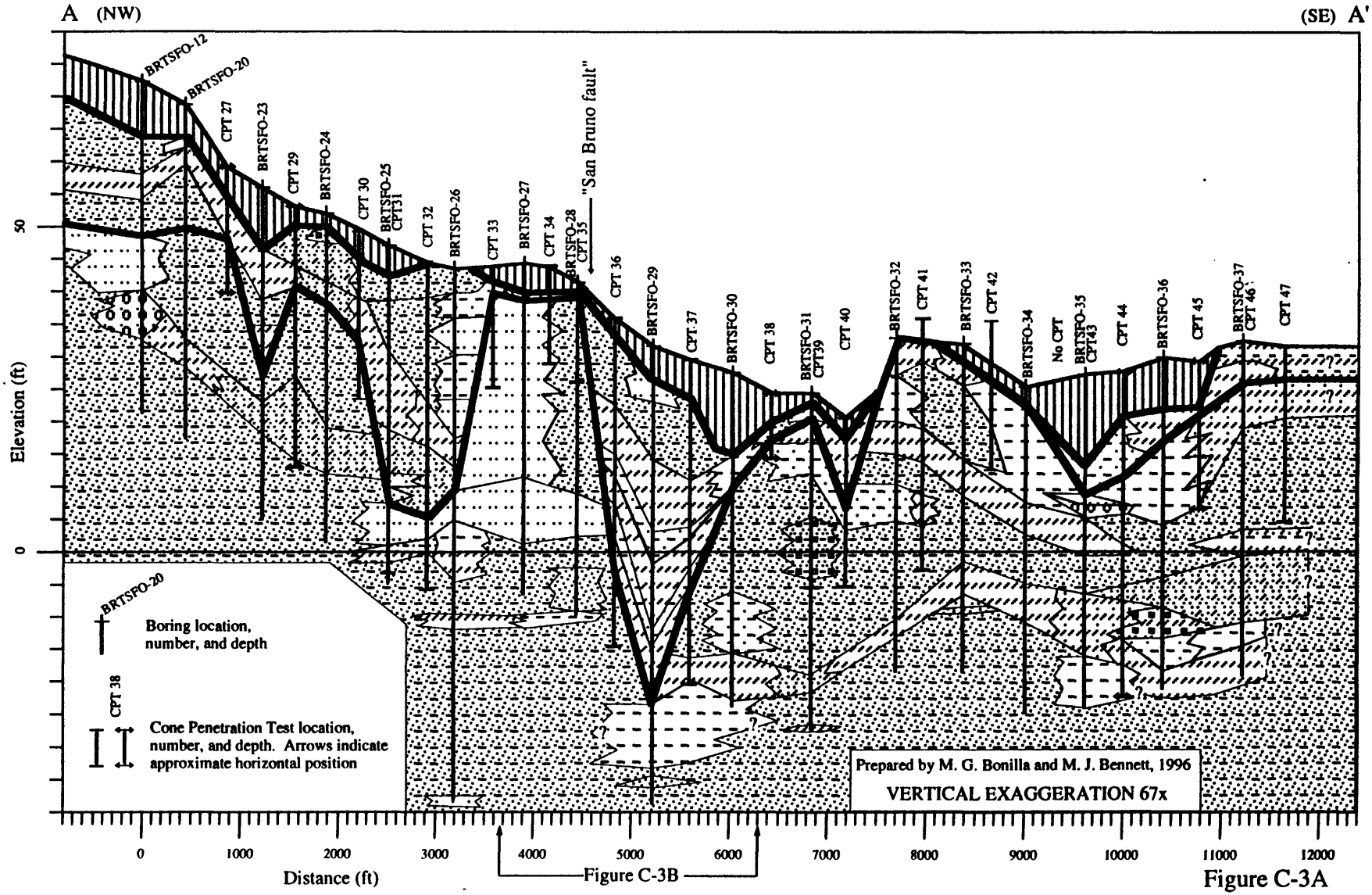
A (NW)
(SE) A'
BRTSFO-12
BRTSFO-20
CPT 27
BRTSFO-23
CPT 29
BRTSFO-24
CPT 30
BRTSFO-25
CPT31
CPT 32
BRTSFO-26
CPT 33
BRTSFO-27
CPT 34
BRTSFO-28
CPT 35
"San Bruno fault"
CPT 36
BRTSFO-29
CPT 37
BRTSFO-30
CPT 38
BRTSFO-31
CPT39
CPT 40
BRTSFO-32
CPT 41
BRTSFO-33
CPT 42
BRTSFO-34
No CPT
BRTSFO-35
CPT43
CPT 44
BRTSFO-36
CPT 45
BRTSFO-37
CPT 46
CPT 47
Elevation (ft)
50
0
BRTSFO-20
Boring location, number, and depth
CPT 38
Cone Penetration Test location, number, and depth. Arrows indicate approximate horizontal position
Prepared by M. G. Bonilla and M. J. Bennett, 1996
VERTICAL EXAGGERATION 67x
0
1000
2000
3000
4000
5000
6000
7000
8000
9000
10000
11000
12000
Distance (ft)
Figure C-3B

Figure C-3A

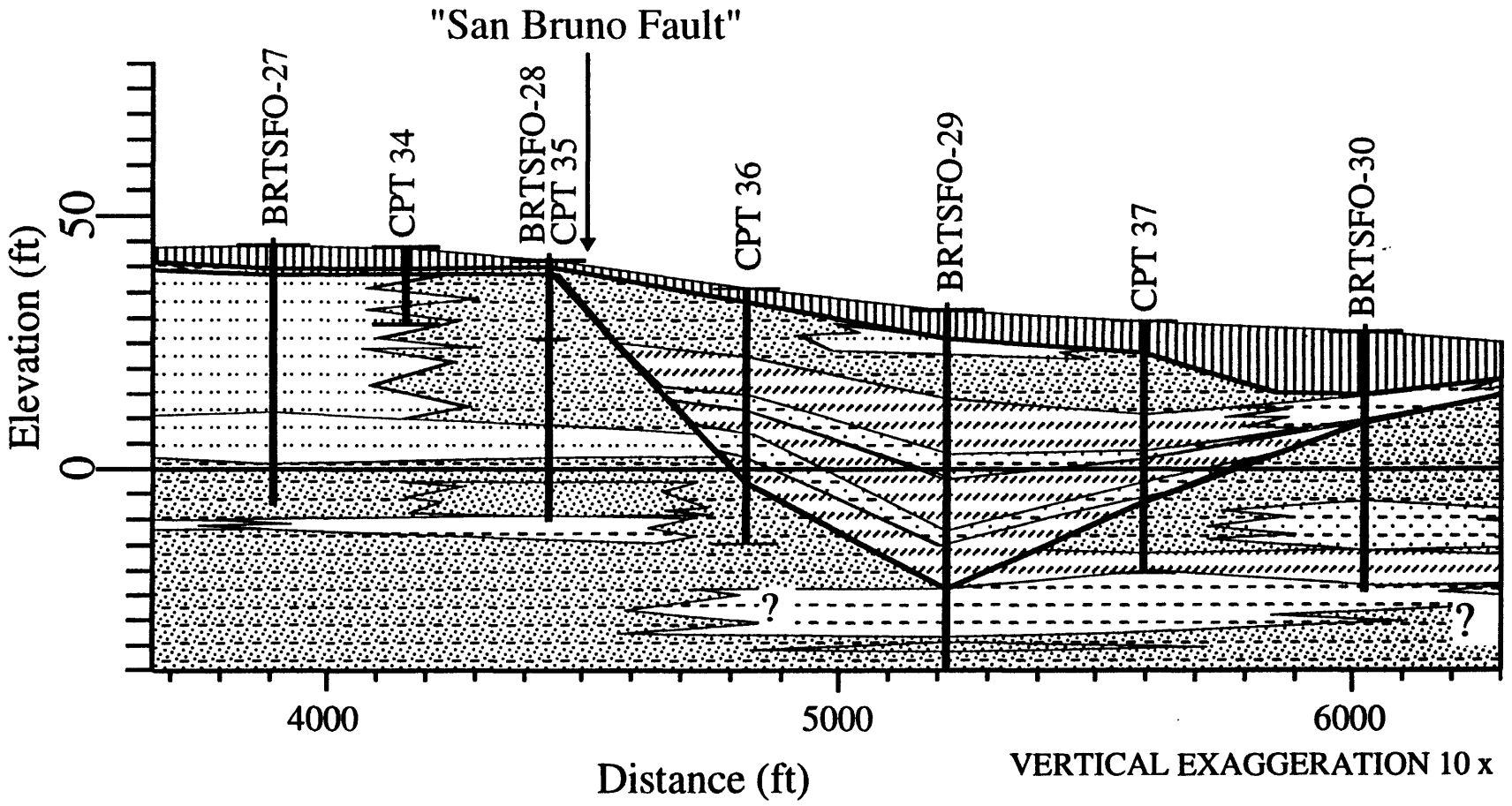

Figure C-3B. Part of section A-A' with smaller (10x) vertical exaggeration.

Figure C-4. Cross section B-B'. Interfingering relations of the slope debris (colluvium) with other unconsolidated sediments is schematic. Borings above or below apparent ground surface are projected to section line.

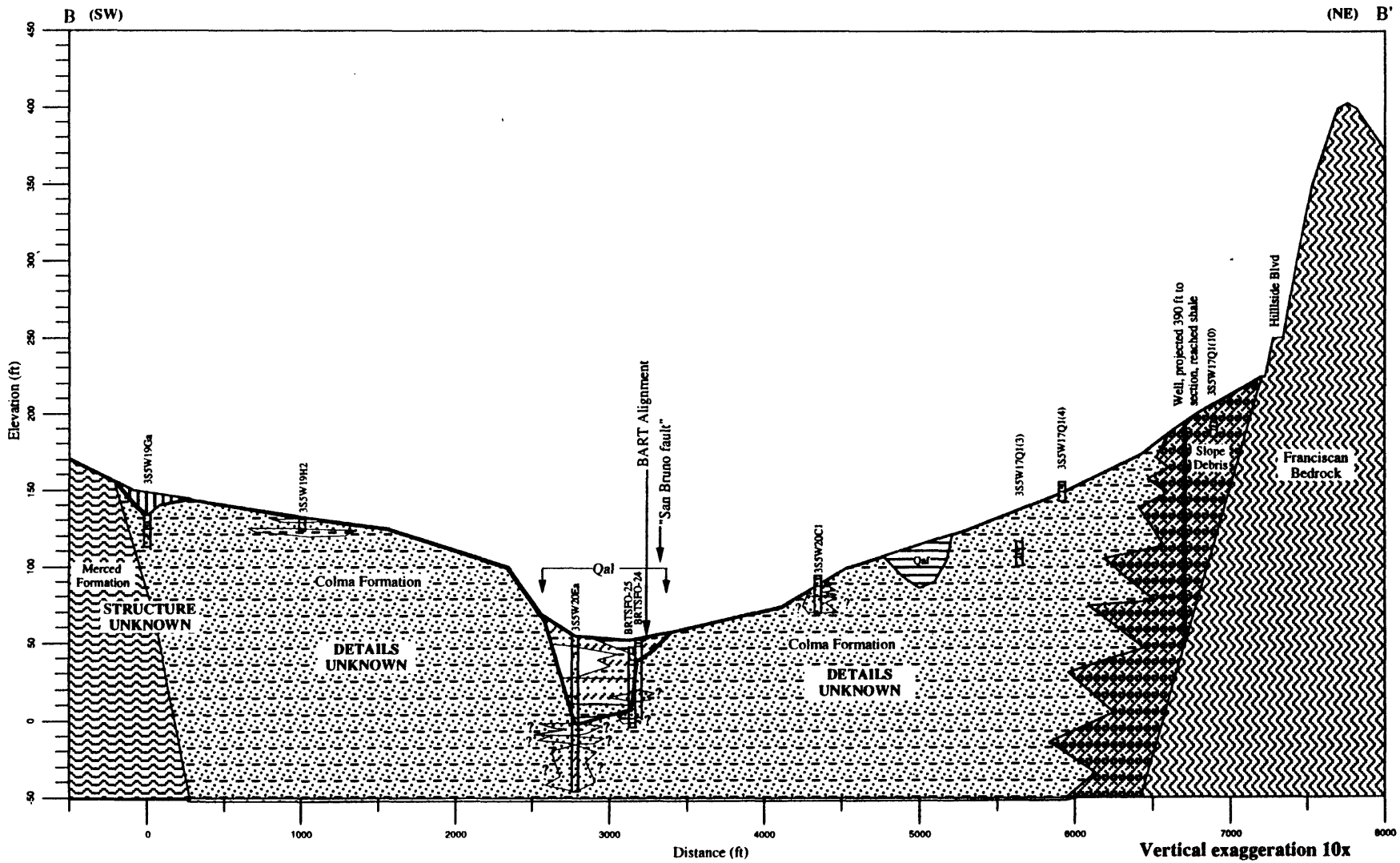
B (SW)
(NE) B'
Elevation (ft)
Distance (ft)
Vertical exaggeration 10x
Merced Formation
STRUCTURE UNKNOWN
Colma Formation
DETAILS UNKNOWN
Qal
BART Alignment
"San Bruno fault"
Colma Formation
DETAILS UNKNOWN
Slope Debris
Franciscan Bedrock
Hillside Blvd
Well, projected 390 ft to section, reached shale
3S/5W/19Ca
3S/5W/19H2
3S/5W/20E2
3S/5W/20C1
3S/5W/17Q1(3)
3S/5W/17Q1(4)
3S/5W/17Q1(10)
BRTSFD-25
BRTSFD-24

Figure C-4

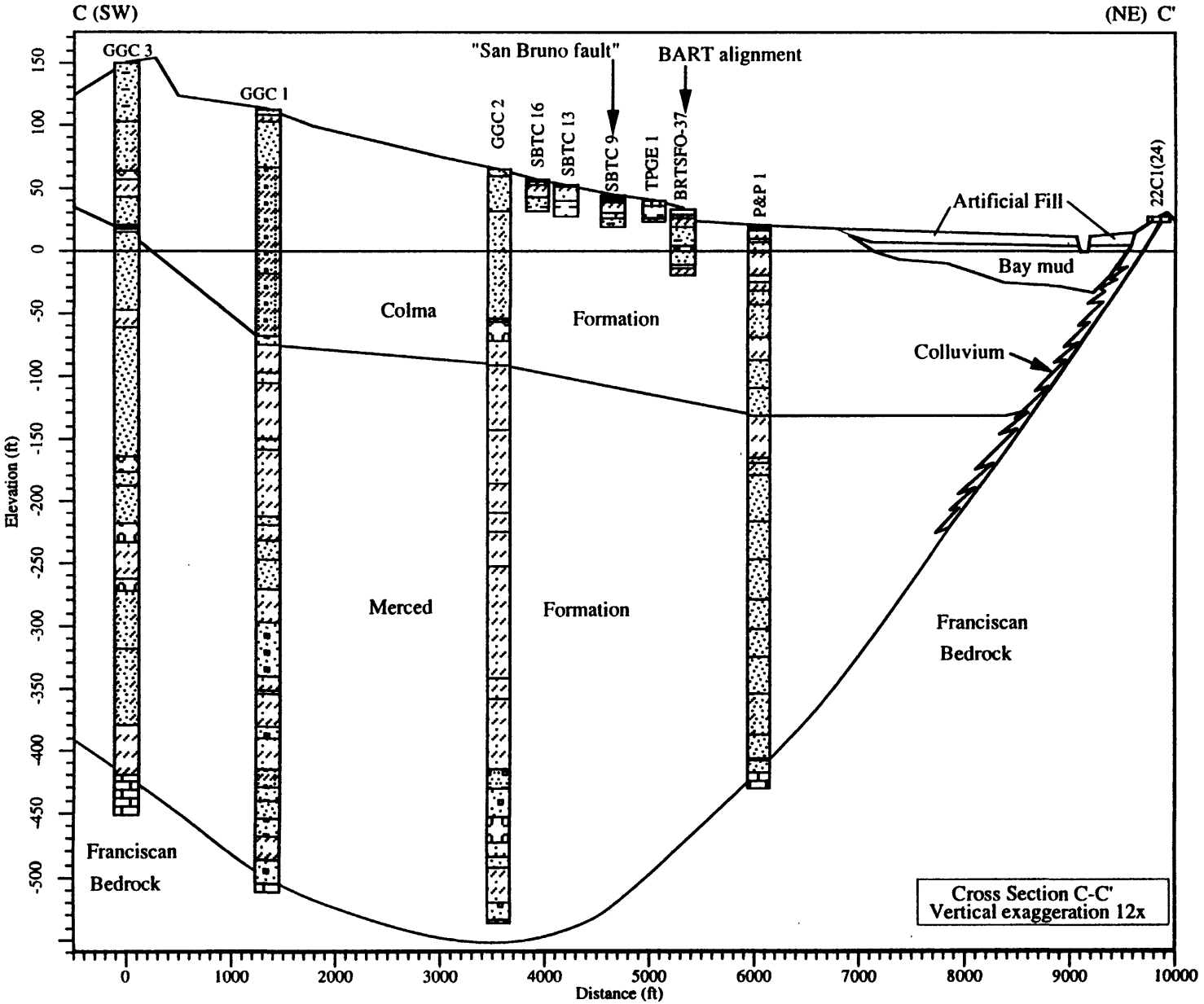

Figure C-5. Cross section C-C'. Colluvium schemattically represented. Vertical exaggeration 12x.

REFERENCES CITED

Baranov, V., 1957, A new method for interpretation of aeromagnetic maps: Pseudo-gravimetric anomalies: Geophysics, v. 22, p. 359-383.

Blakely, R.J., 1995, Potential theory in gravity and magnetic applications: Cambridge University Press, Cambridge U.K., 441 p.

Blakely, R.J., and Simpson, R.W., 1986, Approximating edges of source bodies from magnetic or gravity anomalies: Geophysics, v. 51, p. 1494-1496.

Bonilla, M.G., 1959, Geologic observations in the epicentral area of the San Francisco earthquake of March 22, 1957: California Division of Mines, Special Report 57, p. 25-37.

Bonilla, M.G., 1964, Bedrock-surface map of the San Francisco South quadrangle, California: U.S. Geological Survey Open-File Report, 1:20,000.

Bonilla, M. G., 1965, Geologic map of the San Francisco South quadrangle, California: U.S. Geological Survey Open-File Map, 1:20,000.

Bonilla, M.G., 1971, Preliminary geologic map of the San Francisco South quadrangle and part of the Hunters Point quadrangle, California: U.S. Geological Survey Miscellaneous Field Studies Map MF-311, 2 sheets, scale 1:24,000.

Bonilla, M. G., 1994, Surface faulting studies, p. 241-242 in Jacobson, M.L.(compiler), Summaries of technical reports volume XXXV, prepared by Participants in National Earthquake Hazards Reduction Program, U.S. Geological Survey Open-File Report 94-176.

Brabb, E.E., and Hanna, W.F., 1981, Maps showing aeromagnetic anomalies, faults, earthquake epicenters, and igneous rocks in the southern San Francisco Bay region, California: U.S. Geological Survey Geophysical Investigations Map GP-932, 3 sheets, scale 1:125,000.

Briggs, I.C., 1974, Machine contouring using minimum curvature: Geophysics, v. 39, p. 39-48.

Caldwell-Gonzalez-Kennedy-Tudor, 1982A, Bayside facilities plan, expanded geotechnical investigation, geotechnical reference report: San Francisco, California, Caldwell-Gonzalez-Kennedy-Tudor Consulting Engineers, 127 p.

Caldwell-Gonzalez-Kennedy-Tudor, 1982B, Expanded geotechnical investigation, Element 2: Crosstown Transport Facility, prepared for the City and County of San Francisco. Volume 1, August, 1982.

Caldwell-Gonzalez-Kennedy-Tudor, 1982C, Expanded geotechnical investigation, Element 2: Crosstown Transport Facility, prepared for the City and County of San Francisco. Volume 2: Appendix A, August, 1982.

Caldwell-Gonzalez-Kennedy-Tudor, 1982D, Expanded geotechnical investigation, Element 2: Crosstown Transport Facility, prepared for the City and County of San Francisco, Volume 3: Appendices B through E, August, 1982.

Clifton, H.E., and Hunter, R.E., 1987, The Merced Formation and related beds: A mile-thick succession of late Cenozoic coastal and shelf deposits in the seacliffs of San Francisco, California, in Hill, M.L., Cordilleran Section of the Geological Society of America, Centennial Field Guide, v. 1, p. 257-262.

Cockerham, R.S., McCulloch, D.S., and Greene, H.G., 1990, Earthquake epicenters and selected fault plane solutions of the central California Continental Margin, in Greene, H.G., and Kennedy, M.P., eds., California Continental Margin Geologic Map Series, Central California Continental Margin: California Division of Mines and Geology, Map no. 5B, scale 1:250,000.

Cordell, Lindrith, and Grauch, V.J.S., 1985, Mapping basement magnetization zones from aeromagnetic data in the San Juan basin, New Mexico, *in* Hinze, W.J., ed., The utility of regional gravity and magnetic anomaly maps: Society of Exploration Geophysicists, Tulsa, p. 181-197.

Dobrin, M.B. and Savit, C.H., 1988, Introduction to geophysical prospecting: McGraw- Hill Book Co., New York, N.Y., 867 p.

Geotechnical Consultants, Inc., 1995, Geotechnical Data Report, Segment No. 1, San Francisco Bay Area Rapid Transit District, Proposed SFO Extension, Prepared for Bay Area Transit Consultants, 17 p., 33 figs., 4 appendixes.

Greve, G.M., 1962, An investigation of the earth's gravitational and magnetic fields on the San Francisco Peninsula, California: Ph.D dissertation, Stanford University, Stanford, Calif., 209 p.

Hengesh, J.V., and Wakabayashi, John, 1994, Quaternary deformation along the onshore projection of the Coyote Point fault zone [abs.]: EOS, Transactions, American Geophysical Union, v. 75, no. 44, Supplement, p. 681. (1994 Fall Meeting, San Francisco).

Hengesh, J.V., and Wakabayashi, John, 1995, Quaternary deformation between Coyote Point and Lake Merced on the San Francisco Peninsula: Implications for evolution of the San Andreas fault, in Jacobson, M.L., compiler, National Earthquake Hazards Reduction Program annual project summaries: XXXVI, v.1: U.S. Geological Survey Open-File Report 95-210, p. 417-427.

Hensolt, W.H., and Brabb, E.E., 1990, Maps showing elevation of bedrock and implications for design of engineered structures to withstand earthquake shaking in San Mateo County, California: U.S. Geological Survey Open-File Report 90-496.

Hunter, R. E., Clifton, H.E., Hall, N.T., Csaszar, Geza, Richmond, B.M., and Chin, J.L., 1984, Pleistocene shoreline and shelf deposits at Fort Funston and their relation to sea-level changes: Field Guide , Society Economic Paleontologists and Mineralogists, v. 3, p. 1-30.

Jachens, R.C., Bruns, T.R., Zoback, M.L., and Roberts, C.R., unpub. data, 1996, regarding concealed faults of the San Andreas system, central San Francisco Bay area.

Jachens, R.C., and Moring, B.C., 1990, Maps of the thickness of Cenozoic deposits and the isostatic residual gravity over basement for Nevada: U.S. Geological Survey Open-File Report 90-404, 15 p., 2 sheets, scale 1:1,000,000.

Jachens, R.C., Roberts, C.R., and Zoback, M.L., 1996, Total offset and right-stepping geometry of the San Francisco Peninsula segment of the San Andreas fault, California, defined by aeromagnetic anomalies [abs.]: EOS, Transactions, American Geophysical Union, v. 77, no. 46, Supplement, p. F742.

Jennings, C. W., 1994, Fault Activity map of California and adjacent areas with locations and ages of recent volcanic eruptions: California Division of Mines and Geology, Geologic Data Map No. 6, scale 1:750,000.

Kennedy, M.P., Greene, H.G., and Clarke, S.H, 1987, Geology of the California continental margin: Explanation of the California Continental Margin Geologic Map Series--Interpretive methods, symbology, stratigraphic units, and bibliography: California Division of Mines and Geology Bulletin 207, 110 p.

Lawson, A. C., 1893, The post Pliocene diastrophism of the coast of southern California: University of California Dept. of Geology Bulletin, v. 1, p. 115-160.

Lawson, A. C., 1895, Sketch of the geology of the San Francisco peninsula: U.S. Geological Survey Annual Report 15, p. 399-476.

Lawson, A.C., 1914, San Francisco Folio: Washington, D. C, U.S. Geological Survey Geological Atlas of the United States, Folio 193, 24 p.

Leighton, D.A., Fio, J.L., and Metzger, L.F., 1995, Database of well and areal data, south San Francisco Bay and Peninsula area: U.S.G.S. Water Resources Research Report WRI 94-4251, 47 p.

McCulloch, D.S., and Greene, H.G., 1990, Geologic map of the central California continental margin, in Greene, H.G., and Kennedy, M.P., eds., California Continental Margin Geologic Map Series, Central California Continental Margin: California Division of Mines and Geology, Map 5A, scale 1:250,000.

Pampeyan, E.H., 1994, Geologic map of the Montara Mountain and San Mateo 7-1/2' quadrangles, San Mate County, California: U.S. Geological Survey Miscellaneous Investigations Series Map I-2390, scale 1:24,000.

Roberts, C.W., 1991, Principal facts for more than 700 new gravity stations in the San Francisco North and San Francisco South quadrangles, California: U.S. Geological Survey Open-File Report 91-103, 29 p.

Rubin, Meyer, and Alexander, Corrinne, 1960, U.S. Geological Survey radiocarbon dates V: American Journal of Science Radiocarbon Supplement, v. 2, p. 129-185.

Smith, D.D., 1960, The Geomorphology of part of the San Francisco Peninsula: Ph. D. thesis, Stanford University, 356 p.

Taylor, W. R., 1995, Letter to S.W. Taylor, Regional Administrator, Federal Transit Administration: Washington, U.S. Department of the Interior.

Telford, W.M., Geldart, L.P., Sheriff, R.E., and Keys, D.A., 1976, Applied geophysics: Cambridge University Press, Cambridge U.K., 860 p.

Wentworth, C.M., Bonilla, M.G., and Jayko, A.S., unpub. data, 1996, for a digital elevation map of the 1852 to 1869 U. S. Coast Survey topographic maps of part of the San Francisco Peninsula, California.

Yates, E. B., Hamlin, S. N., and McCann, L. H., 1990, Geohydrology, water quality, and water budgets of Golden Gate Park and the Lake Merced area in the western part of San Francisco, California: U. S. Geological Survey Water-Resources Investigations Report WRI 90-4080, 45 p.

Zoback, M.L., and Jachens, R.C., 1996, Right-stepping geometry of the San Andreas and San Gregorio faults and persistent normal faulting in the 1906 San Francisco earthquake epicentral area [abs.]: EOS, Transactions, American Geophysical Union, v. 77, no. 46, Supplement, p. F742.

Zoback, M.L., and Olson, Jean, 1994, Seismotectonics of the San Francisco Peninsula: p. 736-739 in National Earthquake Hazard Reduction Program, Summaries of Technical Reports, v. XXXV, v. II, U. S. Geological Survey Open-File Report 94-176.

Zoback, M.L., Olson, J.A., and Jachens, R.C., 1995, Seismicity and basement structure beneath south San Francisco Bay, California:, p. 31-46 in Sangines, E.M., Andersen, D.W., and Buising, A.V., eds., Recent geologic studies in the San Francisco Bay Area: Pacific Section, SEPM, Book 76, 278 p.